Genetic evidence for functional diversification of gram-negative intermembrane phospholipid transporters

Ashutosh K. Rai[a], Katsuhiro Sawasato[b], Haley C. Bennett[a], Anastasiia Kozlova[b], Genevieve C. Sparagna[c], Mikhail Bogdanov[b], and Angela M. Mitchell[a,#]

[a] Department of Biology, Texas A&M University, College Station, Texas, USA

[b] Department of Biochemistry and Molecular Biology, McGovern Medical School at The University of Texas Health Science Center at Houston, Houston, Texas, USA

[c] Department of Medicine, Division of Cardiology, University of Colorado Anschutz Medical Campus, Aurora, Colorado, USA

Running title: Phospholipid transporter functional differentiation

Address correspondence to Angela M. Mitchell, amitchell@bio.tamu.edu

Keywords: phospholipid trafficking, gram-negative envelope, outer membrane, lipid metabolism, cold sensitivity

Abstract

The outer membrane of Gram-negative bacteria is a barrier to chemical and physical stress. Phospholipid transport between the inner and outer membranes has been an area of intense investigation and, in *E. coli* K-12, it has recently been shown to be mediated by YhdP, TamB, and YdbH, which are suggested to provide hydrophobic channels for phospholipid diffusion, with YhdP and TamB playing the major roles. However, YhdP and TamB have different phenotypes suggesting distinct functions. We investigated these functions using synthetic cold sensitivity (at 30 °C) caused by deletion of *yhdP* and *fadR*, a transcriptional regulator controlling fatty acid degradation and unsaturated fatty acid production, but not by Δ*tamB* Δ*fadR* or Δ*ydbH* Δ*fadR*,. Deletion of *tamB* suppresses the Δ*yhdP* Δ*fadR* cold sensitivity suggesting this phenotype is related to phospholipid transport. The Δ*yhdP* Δ*fadR* strain shows a greater increase in cardiolipin upon transfer to the non-permissive temperature and genetically lowering cardiolipin levels can suppress cold sensitivity. These data also reveal a qualitative difference between cardiolipin synthases in *E. coli*, as deletion of *clsA and clsC* suppresses cold sensitivity but deletion of *clsB* does not despite lower cardiolipin levels. In addition to increased cardiolipin, increased fatty acid saturation is necessary for cold sensitivity and lowering this level genetically or through supplementation of oleic acid suppresses the cold sensitivity of the Δ*yhdP* Δ*fadR* strain. Although indirect effects are possible, we favor the parsimonious hypothesis that YhdP and TamB have differential substrate transport preferences, most likely with YhdP preferentially transporting more saturated phospholipids and TamB preferentially transporting more unsaturated phospholipids. We envision cardiolipin contributing to this transport preference by sterically clogging TamB-mediated transport of saturated phospholipids. Thus, our data provide a potential mechanism for independent control of the phospholipid composition of the inner and outer membranes in response to changing conditions.

Author Summary

Gram-negative bacteria possess a highly impermeable outer membrane, which protects against environmental stress and antibiotics. Outer membrane phospholipid transport remained mysterious until YhdP, TamB, and YdbH were recently implicated in phospholipid transport between the inner and outer membranes of *E. coli*. Similar roles for YhdP and/or TamB have been suggested in both closely and distantly related gram-negative bacteria. Here, given the transporters' apparent partial redundancy, we investigated functional differentiation between YhdP and TamB. Our data suggest YhdP and TamB have differential involvement with fatty acid and phospholipid metabolism. In fact, transport of higher than normal levels of cardiolipin and saturated phospholipids in the absence of YhdP and presence of TamB at a non-permissive temperature is lethal. We suggest a model where the functions of YhdP and TamB are distinguished by phospholipid transport preference with YhdP preferentially transporting more saturated phospholipids and TamB more unsaturated phospholipids. Cardiolipin headgroup specificity may contribute transport inhibition due to its bulky nature inhibiting the passage of other phospholipids. Diversification of function between YhdP and TamB provides a mechanism for regulation of phospholipid composition, and possibly the mechanical strength and permeability of the outer membrane, and so the cell's intrinsic antibiotic resistance, in changing environmental conditions.

Introduction

The gram-negative bacterial cell envelope has an outer membrane (OM) that sits outside the aqueous periplasm and peptidoglycan cell wall. The OM provides a barrier against various environmental stresses including toxic molecules such as antibiotics and osmotic pressure (1-6). Unlike the inner membrane (IM), a phospholipid bilayer, the OM is largely composed of phospholipids (mainly phosphatidylethanolamine (PE) (7)) in its inner leaflet and LPS (lipopolysaccharide) in its outer leaflet (2, 8). However, both membranes are asymmetric as the IM has different phospholipid compositions in its inner versus outer leaflets (9). Outer membrane proteins (OMPs) form a network across the cell surface interspersed with phase separated LPS patches (10). Lipoproteins are generally anchored in the inner (i.e., periplasmic) leaflet of the OM (11).

OM components are synthesized in the cytoplasm or IM and transported to the OM. OMP (12), lipoprotein (11), and LPS (13) transport pathways are well defined. However, until recently, intermembrane phospholipid transport (between the IM and OM), especially anterograde transport from the IM to the OM, has remained very poorly understood. Phospholipids are synthesized at the IM's inner leaflet (14) and rapid, bidirectional intermembrane phospholipid transport occurs (15), even without ATP (16). Phospholipid transport has a relaxed specificity, allowing transport of non-native lipids (17, 18); however, intermembrane phospholipid composition differences are maintained (7, 19-22). For instance, the OM is enriched for PE and its saturated species compared to the IM outer leaflet (7, 9, 20-22); however, phosphatidylglycerol (PG) and cardiolipin (CL) can be evenly distributed between the IM and OM when the cellular level of PE is greatly reduced (17), suggesting a maintenance of membrane charge balance. This headgroup redistribution is accompanied by a concomitant fatty acid redistribution evidenced by an accumulation of palmitic acid (C16:0) and cyclopropane derivatives of palmitoleic acid (C16:1) and *cis*-vaccenic acid (C18:1). In contrast, the 1,2-diglyceride that accumulates in mutants lacking DgkA (diglyceride kinase) predominantly associates with the IM (23), suggesting existence of a mechanism of discrimination of lipid transfer to the OM that does not recognize diglyceride molecules and contributes to the diversification of distribution of polar and acyl groups between the IM and OM. This establishment and maintenance of defined lipid topography between the IM and the OM must involve the coordinated biosynthesis and balanced bidirectional trafficking of specific phospholipids across the IM and from the IM to the OM (24).

It has been demonstrated that anterograde phospholipid transport is mediated by a high-flux, diffusive (i.e., concentration gradient, not energy dependent) system in *Escherichia coli* (25). A retrograde trafficking pathway, the Mla system, removes mislocalized phospholipids from the OM outer leaflet and returns them to the IM (26). A gain-of-function allele, *mlaA** (27, 28), opens a channel allowing phospholipids to mislocalize to the cell surface by flowing from the OM's inner to outer leaflet (27, 29), resulting in a PldA (OM phospholipase A)-mediated attempt to reestablish OM

112 asymmetry by increasing LPS production, OM vesiculation, and increased flow of
113 phospholipids to the OM (27, 28). When nutrients are depleted, inhibiting phospholipid
114 production, cells lyse due to loss of IM integrity (16, 18). Single cell imaging of *mlaA**
115 cells confirmed an aberrant lipid flow from the IM to the OM at a fast rate. Loss of YhdP,
116 an inner membrane protein, could significantly slow phospholipid flow to the OM
117 resulting in loss of OM integrity before IM rupture (25), suggesting YhdP might play a
118 role in intermembrane phospholipid transport.

119 Recently, YhdP and two homologs, TamB and YdbH, were demonstrated to be
120 intermembrane phospholipid transporters (30, 31). Ruiz, *et al*. investigated AsmA family
121 proteins and found Δ*yhdP* Δ*tamB* mutants showed synthetic OM permeability and
122 stationary phase lysis (30). Moreover, when combined, Δ*yhdP*, Δ*tamB*, and Δ*ydbH* are
123 synthetically lethal. Genetic interactions of these mutants with *mlaA* and *pldA* show
124 their involvement in OM phospholipid homeostasis. Predicted structures of YhdP, TamB,
125 and YdbH (32, 33), as well as a partial crystal structure of TamB (34), have a β-taco fold
126 domain with a hydrophobic pocket, resembling eukaryotic lipid transporters (35-38).
127 These structural findings are another clue that suggests YhdP, TamB, and YdbH are
128 involved in phospholipid transport. Douglass, *et al.* confirmed the synthetic lethality of
129 Δ*yhdP*, Δ*tamB*, and Δ*ydbH* and demonstrated a Δ*tamB* Δ*ydbH* mutant with reduced
130 *yhdP* expression had decreased amounts of OM phospholipids, directly demonstrating
131 their involvement in intermembrane phospholipid transport or its regulation (31).
132 Structural studies have shown that YhdP is long enough to span the periplasmic space
133 and molecular dynamics indicate that the C-terminus of YhdP can insert into the OM to
134 allow phospholipid transfer between the membranes (39). This study also directly
135 demonstrates that a phosphate containing substrate, putatively assigned to be
136 phospholipids, can be crosslinked to the hydrophobic groove of YhdP (39). The role of
137 YhdP, TamB, and YdbH in phospholipid transport may be widely conserved as recent
138 evidence implicates TamB in anterograde phospholipid transport in *Veillonella parvula*,
139 a diderm Fermicute (40) and YhdP, TamB, YdbH, and PA4735 in intermembrane
140 phospholipid transport in *Pseudomonas aeruginosa* (41).

141 Nevertheless, why there are three separate intermembrane phospholipid transport
142 proteins and the functional interactions between these proteins remains unanswered,
143 although it is clear the proteins are not fully redundant or functionally equivalent. The
144 conditional expression of *yhdP* alone, without the presence of *ydbH* and *tamB*, fully
145 complements neither growth phenotypes nor a normal level of OM phospholipids,
146 suggesting transport function is still impaired in this strain (31). In addition, YdbH seems
147 to play a more minor role than YhdP and TamB (30, 31) and the screen identifying Δ*yhdP*
148 as slowing *mlaA**-dependent lysis did not identify Δ*tamB* or Δ*ydbH* (25). Moreover, we
149 previously identified a role for YhdP in stationary phase SDS (sodium dodecyl sulfate)
150 resistance and modulating cyclic enterobacterial common antigen activity (42, 43) not
151 shared by TamB and YdbH (**Fig. S1AB**) (30, 31, 42, 43). Similarly, TamB, in conjunction

with TamA, has been suggested to play a role in OM insertion of some "complicated" β-barrel OMPs such as autotransporters and usher proteins (34, 44-46).

Here, we investigated the differentiation of YhdP and TamB function and identified synthetic cold sensitivity in a strain with Δ*yhdP* and Δ*fadR*, a transcriptional regulator of fatty acid biosynthesis and degradation, acting as a transcriptional switch between these pathways in response to acyl-CoA (47). FadR is necessary for normal levels of unsaturated fatty acids to be synthesized (48). The cold sensitivity was unique to the Δ*yhdP* Δ*fadR* strain and was suppressed by loss of TamB, demonstrating that the sensitivity is related to phospholipid transport. We found that the Δ*yhdP* Δ*fadR* mutant had a greater increase in levels of a specific phospholipid, cardiolipin (CL) during growth at the non-permissive temperature, and decreasing CL suppressed cold sensitivity. Furthermore, increasing unsaturated fatty acid levels suppressed cold sensitivity. Overall, our data are consistent with a model where TamB and YhdP transport functions are differentiated based on phospholipid fatty acid saturation state, with TamB transporting more unsaturated phospholipids and YhdP transporting more saturated phospholipids, although indirect effects may contribute to the phenotype. Phospholipid species or head group can also contribute to transport specificity, since higher levels of dianionic CL are necessary for the cold sensitivity phenotype, potentially due to functional inhibition of TamB by clogging of its hydrophobic groove.

Results

Loss of FadR and YhdP results in cold sensitivity suppressed by loss of TamB. To investigate YhdP-TamB function differentiation, we created a Δ*yhdP* Δ*fadR* strain, as FadR is a major regulator of lipid homeostasis (47). A deletion strain of *fadR* alone is expected to have decreased fatty acid synthesis, increased fatty acid degradation, and increased fatty acid saturation (47, 48). Surprisingly, Δ*yhdP* Δ*fadR* cultures grown at 30 °C lagged for more than 8 hours, followed by highly variable growth, suggesting suppressor outgrowth (**Fig.1A**). The growth defect was decreased at 37 °C and completely absent at 42 °C. To confirm this cold sensitivity, we estimated efficiency of plating (EOP) and confirmed the severe cold intolerance of the Δ*yhdP* Δ*fadR* strain (5 logs at 30 °C and 3 logs at 37 °C) (**Fig. 1B**). Although, enterobacterial common antigen is necessary for Δ*yhdP*'s OM permeability phenotypes (43), the Δ*yhdP* Δ*fadR* strain's cold sensitivity was unchanged when enterobacterial common antigen was not present (Δ*wecA*) (49) (**Fig. 1C**).

We hypothesized the Δ*yhdP* Δ*fadR* strain's cold sensitivity was due to impairment of phospholipid transport and expected Δ*tamB* and/or Δ*ydbH* to show similar synthetic phenotypes with Δ*fadR*. However, Δ*fadR* Δ*tamB* and Δ*fadR* Δ*ydbH* strains had no growth defects (**Fig 1D**). Although Δ*ydbH* in the Δ*yhdP* Δ*fadR* strain did not alter cold sensitivity (**Fig. 1E**), Δ*tamB* in the Δ*yhdP* Δ*fadR* background completely suppressed the cold

192 sensitivity (**Fig. 1F**). Consistent with previous observations for Δ*yhdP* Δ*tamB* (30), the
193 Δ*yhdP* Δ*fadR* Δ*tamB* strain was mucoid due to Rcs (regulator of capsule synthesis) stress
194 response activation and colanic acid capsule production. Deleting *rcsB*, an Rcs response
195 regulator, prevented mucoidy but did not affect suppression (**Fig. 1F**). We observed only
196 minimal growth phenotypes at 30 °C in the Δ*yhdP* Δ*fadR* Δ*tamB* strain (**Fig. 1G**), similar
197 to those of Δ*yhdP* Δ*tamB* (**Fig. S1C**). Thus, although Δ*fadR* does not suppress Δ*yhdP*
198 Δ*tamB* phenotypes, these data make slow growth an unlikely suppression mechanism.
199 Together, these data suggest the Δ*yhdP* Δ*fadR* strain has impaired phospholipid
200 transport leading synthetic cold sensitivity, which can be relieved by deletion of Δ*tamB*,
201 shifting phospholipid transport to YdbH or causing some regulatory change.

202 We next looked for envelope homeostasis alterations in the Δ*yhdP* Δ*fadR* strain. To
203 identify cell lysis and/or severe OM permeability defects at 30 °C, we assayed CPRG
204 (chlorophenol red-β-D-galactopyranoside) processing. CPRG must contact LacZ in the
205 cytoplasm or supernatant to release chlorophenol red (50). Compared to wild type or
206 single mutants, the Δ*yhdP* Δ*fadR* strain had increased CPRG processing (**Fig. S2A**),
207 demonstrating lysis or increased envelope permeability. When we assayed resistance to
208 molecules excluded by the OM (1, 42, 43, 51, 52) at 37 °C, a semi-permissive
209 temperature, the Δ*yhdP* Δ*fadR* strain showed sensitivity to vancomycin, a large scaffold
210 antibiotic, and SDS EDTA compared to single mutants (**Fig. S2B**). However, with
211 bacitracin treatment or EDTA treatment alone, the Δ*yhdP* Δ*fadR* strain phenocopied the
212 Δ*fadR* single deletion (**Fig. S2CD**). LPS levels were not altered in the Δ*yhdP*, Δ*fadR*,
213 Δ*yhdP* Δ*fadR* or Δ*yhdP* Δ*fadR* Δ*tamB* strains (**Fig. S2E**). OM asymmetry mutations (i.e.,
214 Δ*pldA*, Δ*mlaA*) (26-28, 53) did not have suppressive or synthetic effects on cold
215 sensitivity in the Δ*yhdP* Δ*fadR* strain (**Fig. S3AB**), cold sensitivity is not due to OM
216 asymmetry or the loss thereof. Overall, the changes in OM permeability did not seem
217 sufficient to cause lethality at lower temperature, suggesting the phospholipid transport
218 disruption affects both IM and OM integrity.

219 **Lowering cardiolipin suppresses cold sensitivity.** We investigated phospholipid
220 composition of the wild-type, Δ*yhdP*, Δ*fadR*, and Δ*yhdP* Δ*fadR* strains grown at the
221 permissive temperature (42 °C) to log phase then downshifted to 30 °C. *E. coli*
222 phospholipid composition is generally 75% phosphatidylethanolamine (PE), 20%
223 phosphatidylglycerol (PG), and 5% cardiolipin (CL) with CL increasing in stationary phase
224 (14, 54). Of the three CL synthases, ClsA and ClsB synthesize CL from two PG molecules,
225 while ClsC synthesizes CL from one PG and one PE molecule, so CL and PG levels are
226 generally reciprocally regulated (55-58). For all strains, the levels of PE were similar (**Fig.
227 2A**, **Fig. S4A**). However, the Δ*yhdP* Δ*fadR* strain had increased CL and concomitant
228 decreased PG compared to the wild-type strain and compared to individual Δ*yhdP* and
229 Δ*fadR* mutants (**Fig. 2B**). PgsA synthesizes phosphatidylglycerol-phosphate and is the
230 first enzyme differentiating PG and PE biosynthesis. PgsA depletion would decrease
231 both PG and CL levels, reversing increased CL levels and exacerbating decreased PG
232 levels in the Δ*yhdP* Δ*fadR* strain. We tested the effect of PgsA depletion in a strain

233 background (Δ*rcsF* Δ*lpp*) where *pgsA* is non-essential (59-62). When *pgsA* expression
234 was repressed (glucose panel), the Δ*yhdP* Δ*fadR* cold sensitivity was partially suppressed
235 (**Fig. 2C**), demonstrating that decreased PG does not cause cold sensitivity and
236 suggesting increased CL may be necessary for cold sensitivity. The partial suppression
237 may be due to incomplete depletion of PG and CL or the adaptive response of a cell
238 containing only PE in its membrane. Induction of *pgsA* (arabinose panel) reversed the
239 suppression. The cold sensitivity of the Δ*yhdP* Δ*fadR* strain was lost when CL was fully
240 depleted due to deletion of the genes for all cardiolipin syntheses (Δ*clsABC*) or of the
241 gene for the primary cardiolipin synthase (Δ*clsA*) responsible for CL synthesis in
242 exponential phase (**Fig. 2ADE**, **Fig. S4B**). A decrease in LPS levels is not responsible for
243 the suppression as LPS levels did not change in the Δ*yhdP* Δ*fadR* Δ*clsA* strain (Δ*yhdP*
244 Δ*fadR* Δ*tamB*). Δ*clsB* caused a smaller decrease in CL levels, while Δ*clsC* did not cause a
245 decrease (**Fig. 2AB**, **Fig. 4B**). Surprisingly, however, Δ*clsC* completely suppressed the
246 cold sensitivity, while Δ*clsB* did not (**Fig. 2FG**). Thus, increased CL is necessary for cold
247 sensitivity but CL levels alone cannot explain the phenotype: another factor, such as a
248 specific molecular form (e.g., acyl chain length, saturation state, symmetry of acyl chain
249 arrangement) or localization (e.g., poles vs. midcell or inner vs. outer leaflet) of CL, is
250 required.

251 **Increased *fabA* expression suppresses cold sensitivity.** To identify other factors
252 involved in the cold sensitivity, we applied a forward genetic approach by isolating
253 spontaneous suppressor mutants capable of growing at 30 °C and identified a
254 suppressor mutant (Suppressor 1) that restored growth at 30 °C (**Fig. 3A**), decreased
255 CPRG processing (**Fig. S2A**), and had very similar CL levels (**Fig. 2AB**, **Fig. S4A**) and LPS
256 levels (**Fig. S2**) to the Δ*yhdP* Δ*fadR* strain. We identified a point mutation in the *fabA*
257 promoter region in Suppressor 1 (**Fig. 3B**) and confirmed this mutation was sufficient for
258 suppression (**Fig. 3C**). FabA is a dehydratase/isomerase that introduces *cis* unsaturation
259 into fatty acids (14, 63) and *fabA* is expressed from two promoters controlled by FadR
260 and FabR (64, 65). FadR activates *fabA* expression, while FabR represses. Thus, *fadR*
261 deletion would be expected to lower *fabA* expression. The suppressor mutation was
262 located in the *fabA* promoter FabR binding site (**Fig. 3B**) and we hypothesized this
263 mutation would increase *fabA* expression. *fabA* mRNA levels were more than 4-fold
264 lower in the Δ*yhdP* Δ*fadR* strain than the wild-type strain (**Fig. 3D**). While lower than
265 wild type, the suppressor mutant increased *fabA* mRNA 1.6-fold over the Δ*yhdP* Δ*fadR*
266 strain.

267 We constructed luciferase reporter plasmids with the wild-type *fabA* promoter region or
268 the *fabA* promoter region containing the suppressor mutation. The reporter with the
269 mutated promoter had higher activity in a wild-type, Δ*fadR,* and Δ*fabR* background (**Fig.**
270 **3E**). *fabA* transcription occurs from a promoter downstream of the FabR binding site
271 (65-67). However, when *fadR* is deleted, transcription shifts to the FabR-regulated
272 promoter within the FabR binding region (65-67). Thus, our data indicate the Suppressor
273 1 mutation regulates the constitutive activity of the promoter located in the FabR

274 binding site rather than the affinity of FabR binding. To confirm the effect of changing
275 the second promoter's activity, we tested the effect of Δ*fabR* on cold sensitivity in the
276 Δ*yhdP* Δ*fadR* strain and observed partial suppression (**Fig. S5**). The smaller effect of
277 Δ*fabR* compared to Suppressor 1 may result from other gene expression changes or to
278 the smaller relative effect of Δ*fabR* on *fabA* expression (**Fig. 3E**). Overall, these data
279 demonstrate increasing *fabA* expression, which is necessary for unsaturated fatty acid
280 biosynthesis, rescues cold sensitivity in the Δ*yhdP* Δ*fadR* strain without changing CL
281 levels.

282 **Increasing unsaturated fatty acids relieves cold sensitivity.** Given the effect of *fabA*
283 expression on the Δ*yhdP* Δ*fadR* cold sensitivity, we used liquid chromatography-
284 electrospray ionization mass spectrometry (LC/MS) to characterize the strains'
285 phospholipid saturation state (**Dataset S1**, **Fig. 4A-C, Fig. S6**). Representative spectra
286 demonstrating relative phospholipid composition are shown in **Fig. S7**. As expected,
287 Δ*fadR* caused increased fully saturated and monounsaturated PE and PG with a
288 concomitant decrease of diunsaturated PE (**Fig. 4AB, S6AB**). Similarly, the Δ*fadR* strain
289 demonstrated increased monounsaturated CL with a concomitant decrease in
290 triunsaturated CL (**Fig. 4C, S6C**). Compared to the Δ*fadR* strain, the Δ*yhdP* Δ*fadR* strain
291 had slightly decreased saturation for all three phospholipids, while still displaying more
292 phospholipid saturation than wild type or Δ*yhdP* strains (**Fig. 4A-C, S6C**). Suppressor 1
293 trended towards decreased saturation of all three phospholipids compared to the Δ*yhdP*
294 Δ*fadR* strain (**Fig. 4A-C, S6C**). We wondered whether the suppression difference
295 between Δ*clsC* and Δ*clsB* resulted from the CL saturation state. However, the Δ*yhdP*
296 Δ*fadR* Δ*clsB* and Δ*yhdP* Δ*fadR* Δ*clsC* strains had very similar CL profiles (**Fig. 4C, S6C**),
297 suggesting another qualitative difference affecting suppression, perhaps CL lateral or
298 inter-leaflet distribution in the cell. These strains also showed similar PE and PG
299 saturation profiles to their Δ*yhdP* Δ*fadR* parent (**Fig. 4AB, S6AB**).

300 We hypothesized increasing unsaturated fatty acids suppresses Δ*yhdP* Δ*fadR* cold
301 sensitivity and performed EOPs for cold sensitivity on media containing an unsaturated
302 fatty acid (oleic acid, C18:1 *cis*-9). Exogenous phospholipids can be taken up by *E. coli*,
303 attached to acyl-CoA, and incorporated into phospholipids (68). Oleic acid addition
304 suppressed the Δ*yhdP* Δ*fadR* strain's cold sensitivity (**Fig. 4D**). Supplementing oleic acid
305 increases unsaturated phospholipids and provides an exogenous fatty acid source. To
306 differentiate between saturation state and fatty acid availability, we compared
307 treatment with oleic acid and saturated stearic acid (C18:0). Only oleic acid, and not
308 stearic acid, suppressed the Δ*yhdP* Δ*fadR* strain's cold sensitivity (**Fig. 4E**), confirming
309 increasing unsaturated fatty acids, not fatty acid availability suppresses.

310 **Suppression causes fatty acid metabolism and stress response alterations.** In wild-type
311 cells, *fabA* overexpression does not change phospholipid saturation levels,
312 demonstrating the FabB enzyme is rate limiting for unsaturated fatty acid biosynthesis
313 (69). We were intrigued that Suppressor 1 altered saturation without directly effecting

314 *fabB* expression. We also wondered whether CL levels in the Δ*yhdP* Δ*fadR* strain are
315 transcriptionally regulated. Thus, we investigated the transcriptional landscape of the
316 wild type, the Δ*yhdP* Δ*fadR*, and Suppressor 1 strains after a 30-minute downshift of
317 growth to 30 °C to determine: (i) whether the Δ*yhdP* Δ*fadR* strain had altered *cls* gene
318 expression; (ii) whether Suppressor 1 had other transcriptional changes; and (iii) why
319 increased *fabA* expression decreased saturation. All differentially expressed genes (>2-
320 fold change, $p<0.05$) are listed in **Dataset S2**. Principle component analysis of these
321 genes showed the closest relation between Δ*yhdP* Δ*fadR* strain and Suppressor 1, while
322 the wild-type strain was more distantly related (**Fig. 5A**, **S8A**). Nevertheless, Suppressor
323 1 was more closely related to wild type than was the Δ*yhdP* Δ*fadR* strain. Most
324 differentially regulated genes between Δ*yhdP* Δ*fadR* and wild type and Suppressor 1 and
325 wild type were upregulated (**Fig. 5BC**, **S8BC**). Many of the most highly regulated genes
326 are FadR-regulon members. The majority of differentially regulated genes in Suppressor
327 1 compared to Δ*yhdP* Δ*fadR* are downregulated (**Fig. 5D, S8D**). These genes are involved
328 in many cellular pathways and likely reflect the decreased cellular stress (**Table S2**).
329 Indeed, many external stress response genes are more enriched in Δ*yhdP* Δ*fadR* than in
330 Suppressor 1 (**Fig. S9A**).

331 No significant expression changes occurred in the CL biosynthesis pathway (**Fig. 5E**) or
332 other phospholipid biosynthesis genes (**Fig. S9B**). The increased cardiolipin in Δ*yhdP*
333 Δ*fadR* and Suppressor 1 may be post-transcriptional or due to a change in a regulatory
334 pathway not yet altered after 30 minutes at 30 °C (**Fig. S9C**). Levels of mitochondrial CL
335 can be altered due to differences in substrate binding affinity of the CL synthase based
336 on saturation, with increased saturation decreasing CL synthesis (70), and it may be that
337 a similar pathway operates here, albeit in a different direction. We examined the
338 expression of genes in fatty acid synthesis and degradation, many of which are members
339 of the FadR regulon. In Δ*yhdP* Δ*fadR* compared to wild type, many fatty acid
340 biosynthesis genes significantly decreased while many fatty acid degradation genes
341 significantly increased (**Fig. 5F**), consistent with Δ*fadR* effects. While *fabA* expression is
342 decreased, *fabB* expression is not changed, explaining why increased *fabA* expression
343 causes decreased saturation in Suppressor 1. Overall, our data demonstrate the Δ*yhdP*
344 Δ*fadR* strain's cold sensitivity is due to impaired phospholipid trafficking, and increased
345 phospholipid saturation and cardiolipin are necessary for this functional impairment.

346

347

348 **Discussion**

349 The identification of YhdP, TamB, and YdbH as putative intermembrane phospholipid
350 transporters (30, 31) posed the tantalizing question: why is having three transporters
351 advantageous? Differential phenotypes between the transporters suggest that they
352 possess specialized functions (25, 30, 31, 34, 43-46). Here, we demonstrate each protein
353 plays a distinguishable role in phospholipid transport that can be differentiated based
354 on genetic interactions with lipid metabolism. Disruption of *fadR* and *yhdP* function

355 causes synthetic cold sensitivity not shared by *tamB* or *ydbH*. This sensitivity can be
356 suppressed by removing TamB. This phenotype involves both increased levels of CL and
357 saturated fatty acids, and decreasing amounts of either suppresses. In addition, our data
358 demonstrate that CL synthesized by ClsB and ClsC is qualitatively different—resulting in
359 differential suppression phenotypes—likely due to differences in CL localization, CL-
360 mediated, leaflet-specific changes in lipid packing order (9, 24), localized membrane
361 fluidity (71), or phospholipid transporter interaction.

362 Based on the currently available data, we cannot rule out the possibility that the
363 suppressors we have identified for the Δ*yhdP* Δ*fadR* cold sensitivity act indirectly (e.g.,
364 through regulatory or adaptive changes). However, we now suggest a simple model for
365 the differentiation of function between YhdP and TamB that fully explains our data
366 without invoking additional, more complex interpretations (**Fig. 6A-C**). In this
367 hypothesis, the functions of YhdP and TamB are diversified based on the acyl carbon
368 saturation level preference of the phospholipids they transport: YhdP transports mainly
369 phospholipids with more saturated fatty acids, while TamB transports phospholipids
370 with more unsaturated fatty acids (**Fig. 6A**). Our data and previous data (30, 31) agree
371 YdbH plays a relatively minor role. In the Δ*yhdP* Δ*fadR* strain, YhdP's absence forces
372 more saturated phospholipids to be transported by TamB. At 30 °C, TamB becomes
373 "clogged" by phospholipids having more saturated fatty acyl side chains, impeding
374 transport (**Fig. 6B**). Bulky and intrinsically disordered CL molecules could contribute to
375 the clogging sterically by obstructing the lipid channel and precluding it from
376 translocating other lipid substrates (i.e., PE). We find it interesting that the phenotype of
377 the Δ*yhdP* Δ*fadR* strain is most severe at low temperature, leading to cold sensitivity.
378 This cold-specific effect may occur due to (i) temperature-dependent decreased
379 membrane fluidity and higher lipid packing order involving lower expression of FabF,
380 which is responsible for increased diunsaturated phospholipids at lower temperature
381 (**Fig. 5F**, **Dataset 3**)(14); (ii) higher relative levels of CL (72); (iii) higher amounts of per
382 cell phospholipids at lower temperatures (72) contributing to increased diffusive flow
383 rate; or, (iv) to thermodynamic properties altering TamB transport specificity and/or
384 substrate behavior contributing to efficiency of substrate loading or transport.

385 One interesting aspect of our data is that the presence of TamB, with perhaps inhibited
386 function, causes a worse phenotype than the absence of TamB. Furthermore, the
387 phenotype of a Δ*yhdP* Δ*fadR* Δ*ydbH* strain is not measurably worse than that of the
388 Δ*yhdP* Δ*fadR* strain. Together, these data suggest that YdbH is able to successfully
389 transport phospholipids in the Δ*yhdP* Δ*fadR* strain only when TamB is absent. There are
390 several possible mechanisms for this. The first is that YhdP and TamB are the primary
391 transporters and are the preferred interaction partners for other, as of yet unidentified
392 interaction partners (e.g., putative IM proteins facilitating phospholipid transfer to YhdP
393 and TamB). Another possibility is that there is direct toxicity caused by TamB clogging,
394 perhaps through leaking of micellar phospholipids into the periplasm or through stress
395 response overactivation. A third possibility is that YdbH levels are insufficient in the

396 presence of YhdP and TamB to facilitate phospholipid transport and *ydbH* is upregulated
397 in the absence of the other phospholipid transporters. This will be an interesting area
398 for future investigations.

399 Several pieces of evidence suggest dysregulation of phospholipid transport not just
400 changes to OM phospholipid composition, and so permeability or physical strength,
401 cause the cold sensitivity phenotype of the Δ*yhdP* Δ*fadR* strain. First, the cold sensitivity
402 is unaffected by removing enterobacterial common antigen, which suppresses the
403 membrane permeability of a Δ*yhdP* strain (**Fig. 1C**, (43)), and the OM permeability
404 phenotypes of the Δ*yhdP* Δ*fadR* are not severe (**Fig. S2**). Second, the cold sensitivity is
405 suppressed by deletion of Δ*tamB* (**Fig. 1FG**). Δ*yhdP* Δ*tamB* strains have much greater
406 OM permeability (30) than the Δ*yhdP* or Δ*yhdP* Δ*fadR* strains. Third, CL has been shown
407 to have a normalizing, bidirectional, and leaflet-specific effect on lipid packing order (9,
408 73-76) and membrane fluidity (77-80) opposite of or similar to that of cholesterol,
409 respectively, and so is unlikely to contribute to a phenotype dependent solely on OM
410 membrane fluidity. Thus, the cold sensitivity phenotype correlates with the impairment
411 of phospholipid trafficking and the likely imbalance of phospholipids between the IM
412 and OM and not with the permeability phenotypes of the OM. Nonetheless, it will be
413 useful in the future to conduction comparative analysis of the phospholipid composition
414 of pure IM and OM extracts (i.e., without cross contamination of the other membrane)
415 at both permissive and non-permissive temperatures to directly link the cold sensitivity
416 observed here with changes in phospholipid transport.

417 Although both fatty acid saturation and CL levels affect the Δ*yhdP* Δ*fadR* strain's cold
418 sensitivity, evidence points to saturation rather than headgroup as the main factor
419 separating YhdP and TamB function. Specifically, YhdP loss slows phospholipid transport
420 from the IM to the OM in a *mlaA** mutant, which loses OM material due to vesiculation
421 and lysis when phospholipid biosynthesis is insufficient to replace lost phospholipids
422 (25, 27). CL only accounts for 5% of phospholipids in exponentially growing cells making
423 it unlikely that the loss of CL transport could slow net phospholipid transport to the
424 extent required to slow lysis.

425 Our model suggests the IM and OM saturation state could be independently regulated
426 based on YhdP and TamB activity or levels. IM saturation is regulated by altering the
427 composition of newly synthesized fatty acids, while OM saturation could be separately
428 regulated by allowing increased transport of more saturated or unsaturated
429 phospholipids as necessary. IM and OM acyl saturation has been studied in several
430 strains of *E. coli* and in *Yersinia pseudotuberculosis* (7, 19-21) and higher saturated fatty
431 acid levels were observed in the OM than in the IM, supporting discrimination of
432 phospholipid transport based on saturation. The IM needs to maintain an appropriate
433 level of fluidity to allow IM proteins to fold and diffuse, to allow diffusion of
434 hydrophobic molecules, to regulate cellular respiration, and to maintain membrane
435 integrity (84, 85). However, the OM is a permeability barrier, a load-bearing element

436 that resists turgor pressure (1-6), and has an outer leaflet consisting of LPS (2, 8). LPS
437 has saturated acyl chains and is largely immobile in *E. coli* (86) and a specific
438 phospholipid saturation level may be necessary to match or counterbalance LPS rigidity.
439 OM phospholipids may also play a role in the physical strength of the membrane.
440 Interestingly, previous work has demonstrated that the tensile strength of the OM is
441 lessened in a *yhdP* mutant (25).

442 Possessing two different phospholipid transporters with different saturation state
443 preferences would allow the cell to adapt OM saturation to changing conditions
444 including temperature shifts, chemical and physical insults, or changes in synthesis of
445 other OM components (e.g., LPS or OMPs). A recent study demonstrated in *Y.*
446 *pseudotuberculosis* the difference in saturation levels between the membranes is
447 exaggerated at 37 °C compared to 8 °C (21). Thus, conditions where IM and OM
448 saturation are independently regulated exist and this regulation is likely important for
449 optimum fitness of the cells. Transcriptional regulation of *yhdP* and *tamB* has not been
450 thoroughly explored. It seems likely *yhdP* transcription is quite complex with several
451 promoters and transcriptional termination sites (87-89). *tamB* is predicted to be in an
452 operon with *tamA* (which codes for an OMP necessary for TamB function) and *ytfP* (87,
453 90) and to have a σ^E-dependent promoter (91). The σ^E stress response is activated by
454 unfolded OMP accumulation, and downregulates the production of OMPs and
455 upregulates chaperones and folding machinery (74). It is intriguing to speculate a
456 change in OM phospholipid composition might aid in OMP folding due to altered
457 biophysical properties and/or lipoprotein diffusion. In fact, this could explain the
458 observations that some complicated OMPs fold more slowly in the absence of TamB (34,
459 44-46). Proper phospholipid composition may be necessary for efficient folding of these
460 OMPs, as it is necessary for the correct folding and topology of some IM proteins (73,
461 92-95). Recently, it has been demonstrated that the *tamAB* operon is regulated by
462 PhoPQ in *Salmonella enterica* Serovar Typhimurium and that this regulation helps
463 maintain OM integrity in the acidic phagosome environment, perhaps due to indirect
464 effects on OMP folding (96). Thus, changing environments may necessitate changes in
465 phospholipid composition that can be accomplished through differential TamB and,
466 perhaps YhdP, regulation.

467 The mechanism of phospholipid transfer between the IM and OM has been one of the
468 largest remaining questions in gram-negative envelope biogenesis and has remained an
469 area of intense investigation for decades. Furthermore, given the lack of knowledge of
470 this pathway, the role of phospholipid composition in the permeability barrier of the
471 OM, and so the intrinsic antibiotic resistance of gram-negative bacteria, remains
472 unknown. Recent work has begun to elucidate the intermembrane phospholipid
473 transport pathway by identifying YhdP, TamB, and YdbH as proteins capable of
474 transporting phospholipids between the membranes (25, 30, 31). Our work here
475 suggests that YhdP and TamB may have separate roles in phospholipid transport that
476 are differentiated by their preference for phospholipid saturation states and possibly

477 lipid headgroup. Homologs of YhdP and TamB are found throughout *Enterobacterales*
478 and more distantly related members of the AsmA family are widespread in gram-
479 negative bacteria (97). In fact, TamB has recently been shown to play a role in
480 anterograde intermembrane phospholipid transport in the diderm Firmicute *Veillonella*
481 *parvula* (40, 98) and four AsmA members play a role in phospholipid transport in
482 *Pseudomonas aeruginosa* (41). Structural predictions of YhdP and TamB are strikingly
483 similar between species (32, 33). Given this, it is quite likely similar mechanisms of
484 discrimination in intermembrane phospholipid transfer exist in other species. The data
485 we present here provide a framework for investigation of phospholipid transport and
486 mechanisms differentiating phospholipid transporter function in these species.

487

488

489 **Materials and Methods**

490 **Bacterial strains and Growth Conditions. Table S3** lists the strains used in this study.
491 Most knockout strains were constructed with Keio collection alleles using P1vir
492 transduction (99, 100). New alleles were constructed through λ-red recombineering
493 (101), using the primers indicated in **Table S4**. The FLP recombinase-FRT system was
494 used to remove antibiotic resistance cassettes as has been described (101). *E. coli*
495 cultures were grown in LB Lennox media at 42°C, unless otherwise mentioned. Where
496 noted, LB was supplemented with vancomycin (Gold Biotechnology), bacitracin (Gold
497 Biotechnology), SDS (Thermo Fisher Scientific), EDTA (Thermo Fisher Scientific), oleic
498 acid (Sigma Aldrich), stearic acid (Sigma Aldrich), arabinose (Gold Biotechnology), or
499 glucose (Thermo Scientific). For plasmid maintenance, media was supplemented with 25
500 µg/mL kanamycin (Gold Biotechnology), 10 or 20 µg/mL chloramphenicol (Gold
501 Biotechnology), or 10 µg/mL tetracycline (Gold Biotechnology) as appropriate.

502 **Plasmid construction.** The pJW15-P_{fabA}, and pJW15-P_{fabA}(-19G>A) reporter plasmids
503 were constructed by amplifying the region upstream of *fabA* from -432 bp to +27 bp
504 relative to the annotated transcriptional start site from wild-type MG1655 or
505 Suppressor 1, respectively, using the Overlap-pJW15-*fabA* FP and RP primers (**Table S4**).
506 pJW15 was amplified using primers Overlap-pJW15-*fabA* FP1 and RP1. The pJW15
507 plasmid was a kind of gift from Dr. Tracy Raivio (University of Alberta) (102, 103). The
508 resulting fragments were assembled using HiFi Assembly master mix (New England
509 Biolabs) as per the manufacturer's instructions.

510 **Growth and Sensitivity Assays.** For EOPs assays, cultures were grown overnight, serially
511 diluted, and plated on the indicated media. For *pgsA* depletion, overnight cultures
512 grown in arabinose were washed and diluted 1:100 into fresh LB with 0.2% glucose or
513 arabinose as indicated and grown to OD_{600}=1 before diluting and plating on media with
514 glucose or arabinose respective, as above. EOPs were incubated at 30 °C unless
515 otherwise indicated. Growth curves were performed at the indicated temperature as
516 has been described (43), except that starting cultures for growth curves were grown to

517 early stationary phase before inoculation of growth curves rather than overnight. For
518 CPRG assays (50), strains were streaked on LB plates supplemented with CPRG
519 (40µg/ml) and IPTG (100 µM) incubated overnight at 30°C.

520 **Suppressor isolation and sequencing.** Serially diluted cultures were spread on LB plates
521 and incubated overnight at 30°C. Colonies that grew at 30°C were isolated and
522 rechecked for cold resistance through EOP and growth curves. The suppressors were
523 subjected to whole-genome sequencing to identify potential suppressor mutations.
524 Genomic DNA was isolated from the parent and suppressors using a DNeasy Blood and
525 Tissue Kit (Qiagen) as per the manufacturer's instructions. Library preparation and
526 Illumina sequencing were performed by the Microbial Genome Sequencing Center
527 (MiGS, Pittsburgh, PA, USA). Briefly, Illumina libraries were prepared and the libraries
528 were sequenced with paired-end 151 bp reads on a NextSeq 2000 platform to a read
529 depth of at least 200 Mbp. To identify variants from the reference genome (GenBank:
530 U00096.3), reads were trimmed to remove adaptors and the *breseq* software (version
531 0.35.4) was used to call variants (104). Identified mutations were confirmed with Sanger
532 sequencing. The consensus motif of the FabR binding site of *fabA* was determined using
533 Multiple Em for Motif Elicitation (MEME) tool in the MEME Suite based on the sequence
534 of putative FabR binding sites reported by Feng and Cronan (2011) (64, 105, 106). The
535 ability of the identified P_{fabA} mutation to suppress was confirmed by linking the mutant
536 to *zcb*-3059::Tn*10* (107) and transducing to a clean background.

537 **Lux reporter assays.** Overnight cultures of strains harboring the pJW15-P_{fabA} and pJW15-
538 P_{fabA}(-19G>A) plasmids were sub-cultured at (1:100) into 200 µl of fresh LB broth in a
539 black 96-well plate. The plate was incubated in a BioTek Synergy H1 plate reader and
540 the OD_{600} and luminescence intensity were recorded every 2.5 min for 6 hours as
541 described in previously (103, 108). Each biological replicate was performed in technical
542 triplicate.

543 **RNA-seq.** Overnight cultures grown at 42°C were subcultured 1:100 into fresh media
544 and incubated at 42 °C until an OD_{600} of 0.4. Then, the cultures were shifted to a 30 °C
545 water bath for 30 minutes. 500 µL of each culture was immediately fixed in the
546 RNAprotect Bacteria Reagent (Qiagen) as per the manufacturer's instructions. RNA was
547 purified using the RNeasy Kit (Qiagen) with on-column DNase digestion following the
548 manufacturer's protocol for gram-negative bacteria. Library preparation, Illumina
549 sequencing, and analysis of differentially expressed genes were performed by MiGS.
550 Briefly, samples were treated with RNase free DNase (Invitrogen) and library
551 preparation was performed with the Stranded Total RNA Prep Ligation with Ribo-Zero
552 Plus Kit (Illumina). Libraries were sequenced with 2x50 bp reads on a NextSeq2000
553 (Illumina). Demultiplexing, quality control, and adapter trimming carried out using bcl-
554 convert (Illumina, v3.9.3) and bcl2fastq (Illumina). Read mapping and read
555 quantification were performed with HISAT2 (109) and the featureCounts tool in
556 Subreader (110), respectively. Descriptive statistics of the RNA-seq read data can be

557 found in **Table S1**. The raw RNA-seq data is available in the Sequence Read Archive
558 database (SRA) (https://www.ncbi.nlm.nih.gov/sra, BioProject ID PRJNA965821;
559 Reviewer Access).

560 Raw read counts were normalized using the Trimmed Mean of M values algorithm in
561 edgeR (111) and converted to counts per million. The Quasi-Linear F-Test function of
562 edgeR was used for differential expression analysis. Normalized read values and for all
563 genes as well as differential expression analysis statistics can be found in **Dataset S3**.
564 KEGG pathway analysis was conducted using the *"kegga"* function of limma (112).
565 Expression of genes differentially expressed (greater than 2-fold change and $p<0.05$)
566 was subjected to principle component analysis, and pathway and enrichment analysis
567 using the EcoCyc Omics Dashboard (112).

568 **Lipid extraction and TLC.** For thin layer chromatography (TLC) experiments, cultures
569 were grown in LB with 1 mCi/mL ^{32}P until OD_{600} of 0.6-0.8 at the indicated temperature.
570 For temperature downshift experiments, cells were grown at 42 ^{o}C until OD_{600} of 0.2 and
571 then transferred to 30 ^{o}C for 2 hours. For lipid extraction, cells were pelleted and
572 resuspended in 0.2 mL of 0.5 M NaCl in 0.1 N HCl. Lipids were extracted by first adding
573 0.6 mL of chloroform:methanol (1:2) to create a single-phase solution. After vigorous
574 vortexing for 30 minutes, 0.2 mL of 0.5 M NaCl in 0.1 N HCl was added to convert the
575 single-phase solution to a two-phase solution. After centrifugation at 20 000 x g for 5
576 minutes at room temperature, the lower phase was recovered and used for TLC.
577 Approximately 2,000 cpm of phospholipid extract was subjected to TLC analysis using a
578 HPTLC 60 plate (EMD, Gibbstown, NJ)) developed with either solvent 1:
579 chloroform/methanol/acetic acid [60/25/10] (vol/vol/vol) in **Fig. S4A** or by solvent 2:
580 chloroform/methanol/ammonia/water [65/37.5/3/1] (vol/vol/vol/vol) in **Fig. S4B**.
581 Radiolabeled lipids were visualized and quantified using a Phosphoimager Typhoon FLA
582 9500 (GE). Images were processed and quantified using ImageQuant™ software for
583 scanning and analysis. The phospholipid content is expressed as molecular percentage
584 of the total phospholipids (correcting for the two phosphates per molecule of CL).

585 **Phospholipid composition analysis.** Whole cell lipid extracts were isolated as for TLC
586 temperature downshift experiments without radiolabeling. Absolute amounts of CL, PG,
587 and PE were determined in these lipid extracts using liquid chromatography coupled to
588 electrospray ionization mass spectrometry (LC/MS) in an API 4000 mass spectrometer
589 (Sciex, Framingham, MA, USA) using normal phase solvents as previously published
590 (113). The cardiolipin internal standard $(14{:}0)_4$CL (Avanti Polar Lipids, Alabaster, AL USA)
591 was added to all samples to quantify CL, PG, and PE within a single run. Standard curves
592 containing reference standards of all three phospholipids, $(18{:}1)_4$CL (Avanti Polar Lipids),
593 $16{:}0_1 18{:}1_1$PG and $16{:}0_1 18{:}1_1$PE (Cayman Chemicals, Ann Arbor, MI, USA) were used to
594 quantify the nmol/mg protein for each species (**Dataset 1**) as previously described (114).
595 Percentage values were calculated by dividing the absolute value of that species by the

596 sum of individual molecular species of CL, PG, or PE. The identities of CL species were
597 confirmed using tandem mass spectrometry.
598
599
600 **Acknowledgments**
601
602 We thank members of the Mitchell Lab for productive discussions. We would like to
603 thank Professor Tracy Raivio (University of Alberta) for the kind gift of pJW15 plasmid.
604 This work was funded by the National Institute of Allergy and Infectious Disease under
605 Award Number R01-AI155915 and R01-AI155915-S1 (to A.M.M.), the National Institute
606 of General Medical Sciences under Award Number R01-GM121493 (to M.B.), and Texas
607 A&M University start-up funds (to A.M.M.).
608
609
610 **References**

611 1. Nikaido H. Molecular basis of bacterial outer membrane permeability revisited.
612 Microbiology and Molecular Biology Reviews. 2003;67(4):593-656.
613 2. Silhavy TJ, Kahne D, Walker S. The bacterial cell envelope. Cold Spring Harbor
614 Perspectives in Biology. 2010;2(5).
615 3. Henderson JC, Zimmerman SM, Crofts AA, Boll JM, Kuhns LG, Herrera CM, Trent
616 MS. The power of asymmetry: Architecture and assembly of the Gram-negative outer
617 membrane lipid bilayer. Annual Review of Microbiology. 2016;70(1):255-78.
618 4. Berry J, Rajaure M, Pang T, Young R. The spanin complex is essential for lambda
619 lysis. J Bacteriol. 2012;194(20):5667-74.
620 5. Rojas ER, Billings G, Odermatt PD, Auer GK, Zhu L, Miguel A, et al. The outer
621 membrane is an essential load-bearing element in Gram-negative bacteria. Nature.
622 2018;559(7715):617-21.
623 6. Navarro Llorens JM, Tormo A, Martinez-Garcia E. Stationary phase in gram-
624 negative bacteria. FEMS Microbiol Rev. 2010;34(4):476-95.
625 7. Lugtenberg EJJ, Peters R. Distribution of lipids in cytoplasmic and outer
626 membranes of *Escherichia coli* K12. Biochimica et Biophysica Acta (BBA) - Lipids and
627 Lipid Metabolism. 1976;441(1):38-47.
628 8. Kamio Y, Nikaido H. Outer membrane of *Salmonella typhimurium*: accessibility of
629 phospholipid head groups to phospholipase c and cyanogen bromide activated dextran
630 in the external medium. Biochemistry. 1976;15(12):2561-70.
631 9. Bogdanov M, Pyrshev K, Yesylevskyy S, Ryabichko S, Boiko V, Ivanchenko P, et al.
632 Phospholipid distribution in the cytoplasmic membrane of Gram-negative bacteria is
633 highly asymmetric, dynamic, and cell shape-dependent. Science Advances.
634 2020;6(23):eaaz6333.

635 10. Benn G, Mikheyeva IV, Inns PG, Forster JC, Ojkic N, Bortolini C, et al. Phase
636 separation in the outer membrane of *Escherichia coli*. Proceedings of the National
637 Academy of Sciences. 2021;118(44):e2112237118.
638 11. Konovalova A, Silhavy TJ. Outer membrane lipoprotein biogenesis: Lol is not the
639 end. Philosophical Transactions of the Royal Society B: Biological Sciences.
640 2015;370(1679):20150030.
641 12. Konovalova A, Kahne DE, Silhavy TJ. Outer Membrane Biogenesis. Annu Rev
642 Microbiol. 2017;71:539-56.
643 13. Lundstedt E, Kahne D, Ruiz N. Assembly and maintenance of lipids at the
644 bacterial outer membrane. Chemical Reviews. 2021;121(9):5098-123.
645 14. John E. Cronan J, Rock CO. Biosynthesis of membrane lipids. EcoSal Plus.
646 2008;3(1).
647 15. Jones NC, Osborn MJ. Translocation of phospholipids between the outer and
648 inner membranes of *Salmonella typhimurium*. Journal of Biological Chemistry.
649 1977;252(20):7405-12.
650 16. Donohue-Rolfe AM, Schaechter M. Translocation of phospholipids from the inner
651 to the outer membrane of *Escherichia coli*. Proceedings of the National Academy of
652 Sciences. 1980;77(4):1867-71.
653 17. Raetz CR, Kantor GD, Nishijima M, Newman KF. Cardiolipin accumulation in the
654 inner and outer membranes of *Escherichia coli* mutants defective in phosphatidylserine
655 synthetase. J Bacteriol. 1979;139(2):544-51.
656 18. Langley KE, Hawrot E, Kennedy EP. Membrane assembly: movement of
657 phosphatidylserine between the cytoplasmic and outer membranes of *Escherichia coli*. J
658 Bacteriol. 1982;152(3):1033-41.
659 19. White DA, Lennarz WJ, Schnaitman CA. Distribution of lipids in the wall and
660 cytoplasmic membrane subfractions of the cell envelope of *Escherichia coli*. Journal of
661 Bacteriology. 1972;109(2):686-90.
662 20. Ishinaga M, Kanamoto R, Kito M. Distribution of phospholipid molecular species
663 in outer and cytoplasmic membranes of *Escherichia coli*. The Journal of Biochemistry.
664 1979;86(1):161-5.
665 21. Davydova L, Bakholdina S, Barkina M, Velansky P, Bogdanov M, Sanina N. Effects
666 of elevated growth temperature and heat shock on the lipid composition of the inner
667 and outer membranes of *Yersinia pseudotuberculosis*. Biochimie. 2016;123:103-9.
668 22. Osborn MJ, Gander JE, Parisi E, Carson J. Mechanism of Assembly of the Outer
669 Membrane of *Salmonella* typhimurium : Isolation and characterization of cytoplasmic
670 and outer membrane. Journal of Biological Chemistry. 1972;247(12):3962-72.
671 23. Raetz CR, Newman KF. Diglyceride kinase mutants of *Escherichia coli*: inner
672 membrane association of 1,2-diglyceride and its relation to synthesis of membrane-
673 derived oligosaccharides. J Bacteriol. 1979;137(2):860-8.
674 24. Bogdanov M. Renovating a double fence with or without notifying the next door
675 and across the street neighbors: why the biogenic cytoplasmic membrane of Gram-

676 negative bacteria display asymmetry? . Emerging Topics in Life Sciences. 2023;7(1):137-
677 50.
678 25. Grimm J, Shi H, Wang W, Mitchell AM, Wingreen NS, Huang KC, Silhavy TJ. The
679 inner membrane protein YhdP modulates the rate of anterograde phospholipid flow in
680 *Escherichia coli*. Proc Natl Acad Sci U S A 2020;117(43):26907-14.
681 26. Malinverni JC, Silhavy TJ. An ABC transport system that maintains lipid
682 asymmetry in the Gram-negative outer membrane. Proceedings of the National
683 Academy of Sciences. 2009;106(19):8009-14.
684 27. Sutterlin HA, Shi H, May KL, Miguel A, Khare S, Huang KC, Silhavy TJ. Disruption
685 of lipid homeostasis in the Gram-negative cell envelope activates a novel cell death
686 pathway. Proceedings of the National Academy of Sciences. 2016;113(11):E1565-E74.
687 28. May KL, Silhavy TJ. The *Escherichia coli* phospholipase PldA regulates outer
688 membrane homeostasis via lipid signaling. mBio. 2018;9(2):e00379-18.
689 29. Tang X, Chang S, Qiao W, Luo Q, Chen Y, Jia Z, et al. Structural insights into outer
690 membrane asymmetry maintenance in Gram-negative bacteria by MlaFEDB. Nat Struct
691 Mol Biol. 2021;28(1):81-91.
692 30. Ruiz N, Davis RM, Kumar S. YhdP, TamB, and YdbH are redundant but essential
693 for growth and lipid homeostasis of the gram-negative outer membrane. mBio.
694 2021;12(6):e02714-21.
695 31. Douglass MV, McLean AB, Trent MS. Absence of YhdP, TamB, and YdbH leads to
696 defects in glycerophospholipid transport and cell morphology in Gram-negative
697 bacteria. PLOS Genetics. 2022;18(2):e1010096.
698 32. Jumper J, Evans R, Pritzel A, Green T, Figurnov M, Ronneberger O, et al. Highly
699 accurate protein structure prediction with AlphaFold. Nature. 2021;596(7873):583-9.
700 33. Varadi M, Anyango S, Deshpande M, Nair S, Natassia C, Yordanova G, et al.
701 AlphaFold Protein Structure Database: massively expanding the structural coverage of
702 protein-sequence space with high-accuracy models. Nucleic Acids Research.
703 2021;50(D1):D439-D44.
704 34. Josts I, Stubenrauch CJ, Vadlamani G, Mosbahi K, Walker D, Lithgow T, Grinter R.
705 The structure of a conserved domain of TamB reveals a hydrophobic β taco fold.
706 Structure. 2017;25(12):1898-906.e5.
707 35. Kumar N, Leonzino M, Hancock-Cerutti W, Horenkamp FA, Li P, Lees JA, et al.
708 VPS13A and VPS13C are lipid transport proteins differentially localized at ER contact
709 sites. Journal of Cell Biology. 2018;217(10):3625-39.
710 36. Valverde DP, Yu S, Boggavarapu V, Kumar N, Lees JA, Walz T, et al. ATG2
711 transports lipids to promote autophagosome biogenesis. J Cell Biol. 2019;218(6):1787-
712 98.
713 37. Otomo T, Maeda S. ATG2A transfers lipids between membranes *in vitro*.
714 Autophagy. 2019;15(11):2031-2.
715 38. Osawa T, Kotani T, Kawaoka T, Hirata E, Suzuki K, Nakatogawa H, et al. Atg2
716 mediates direct lipid transfer between membranes for autophagosome formation. Nat
717 Struct Mol Biol. 2019;26(4):281-8.

718 39. Cooper BF, Clark R, Kudhail A, Bhabha G, Ekiert DC, Khalid S, Isom GL.
719 Phospholipid transport to the bacterial outer membrane through an envelope-spanning
720 bridge. bioRxiv. 2023:2023.10.05.561070.
721 40. Grasekamp KP, Beaud Benyahia B, Taib N, Audrain B, Bardiaux B, Rossez Y, et al.
722 The Mla system of diderm Firmicute *Veillonella parvula* reveals an ancestral
723 transenvelope bridge for phospholipid trafficking. Nature Communications.
724 2023;14(1):7642.
725 41. Sposato D, Mercolino J, Torrini L, Sperandeo P, Lucidi M, Alegiani R, et al.
726 Redundant essentiality of AsmA-like proteins in *Pseudomonas aeruginosa*. mSphere.
727 2024;9(2):e00677-23.
728 42. Mitchell AM, Wang W, Silhavy TJ. Novel Rpos-dependent mechanisms
729 strengthen the envelope permeability barrier during stationary phase. J Bacteriol.
730 2017;199(2):e00708-16.
731 43. Mitchell AM, Srikumar T, Silhavy TJ. Cyclic enterobacterial common antigen
732 maintains the outer membrane permeability barrier of *Escherichia coli* in a manner
733 controlled by Yhdp. mBio. 2018;9(4):e01321-18.
734 44. Selkrig J, Mosbahi K, Webb CT, Belousoff MJ, Perry AJ, Wells TJ, et al. Discovery
735 of an archetypal protein transport system in bacterial outer membranes. Nature
736 Structural & Molecular Biology. 2012;19(5):506-10.
737 45. Stubenrauch CJ, Dougan G, Lithgow T, Heinz E. Constraints on lateral gene
738 transfer in promoting fimbrial usher protein diversity and function. Open Biology.
739 2017;7(11):170144.
740 46. Stubenrauch C, Belousoff MJ, Hay ID, Shen H-H, Lillington J, Tuck KL, et al.
741 Effective assembly of fimbriae in *Escherichia coli* depends on the translocation assembly
742 module nanomachine. Nature Microbiology. 2016;1(7):16064.
743 47. Cronan JE. The *Escherichia coli* FadR transcription factor: Too much of a good
744 thing? Mol Microbiol. 2021;115(6):1080-5.
745 48. Nunn WD, Giffin K, Clark D, Cronan JE. Role for *fadR* in unsaturated fatty acid
746 biosynthesis in *Escherichia coli*. Journal of Bacteriology. 1983;154(2):554-60.
747 49. Rai AK, Mitchell AM. Enterobacterial common antigen: Synthesis and function of
748 an enigmatic molecule. mBio. 2020;11(4):e01914-20.
749 50. Paradis-Bleau C, Kritikos G, Orlova K, Typas A, Bernhardt TG. A genome-wide
750 screen for bacterial envelope biogenesis mutants identifies a novel factor involved in
751 cell wall precursor metabolism. PLoS Genet. 2014;10(1):e1004056.
752 51. Ruiz N, Falcone B, Kahne D, Silhavy TJ. Chemical conditionality: a genetic strategy
753 to probe organelle assembly. Cell. 2005;121(2):307-17.
754 52. Nikaido H, Vaara M. Molecular basis of bacterial outer membrane permeability.
755 Microbiol Rev. 1985;49(1):1-32.
756 53. Bishop RE. Structural biology of membrane-intrinsic β-barrel enzymes: Sentinels
757 of the bacterial outer membrane. Biochimica et Biophysica Acta (BBA) - Biomembranes.
758 2008;1778(9):1881-96.

759 54. Rowlett VW, Mallampalli V, Karlstaedt A, Dowhan W, Taegtmeyer H, Margolin W,
760 Vitrac H. Impact of membrane phospholipid slterations in *Escherichia coli* on cellular
761 function and bacterial stress adaptation. J Bacteriol. 2017;199(13).
762 55. Tan BK, Bogdanov M, Zhao J, Dowhan W, Raetz CRH, Guan Z. Discovery of a
763 cardiolipin synthase utilizing phosphatidylethanolamine and phosphatidylglycerol as
764 substrates. Proceedings of the National Academy of Sciences. 2012;109(41):16504-9.
765 56. Pluschke G, Hirota Y, Overath P. Function of phospholipids in *Escherichia coli*.
766 Characterization of a mutant deficient in cardiolipin synthesis. Journal of Biological
767 Chemistry. 1978;253(14):5048-55.
768 57. Nishijima S, Asami Y, Uetake N, Yamagoe S, Ohta A, Shibuya I. Disruption of the
769 *Escherichia coli cls* gene responsible for cardiolipin synthesis. Journal of Bacteriology.
770 1988;170(2):775-80.
771 58. Guo D, Tropp BE. A second *Escherichia coli* protein with CL synthase activity.
772 Biochimica et Biophysica Acta (BBA) - Molecular and Cell Biology of Lipids.
773 2000;1483(2):263-74.
774 59. Kikuchi S, Shibuya I, Matsumoto K. Viability of an *Escherichia coli pgsA* null
775 mutant lacking detectable phosphatidylglycerol and cardiolipin. Journal of Bacteriology.
776 2000;182(2):371-6.
777 60. Suzuki M, Hara H, Matsumoto K. Envelope disorder of *Escherichia coli* cells
778 lacking phosphatidylglycerol. Journal of Bacteriology. 2002;184(19):5418-25.
779 61. Shiba Y, Yokoyama Y, Aono Y, Kiuchi T, Kusaka J, Matsumoto K, Hara H.
780 Activation of the Rcs signal transduction system is responsible for the thermosensitive
781 growth defect of an *Escherichia coli* mutant lacking phosphatidylglycerol and cardiolipin.
782 J Bacteriol. 2004;186(19):6526-35.
783 62. Grabowicz M, Silhavy TJ. Redefining the essential trafficking pathway for outer
784 membrane lipoproteins. Proceedings of the National Academy of Sciences.
785 2017;114(18):4769-74.
786 63. Cronan JE, Jr., Gelmann EP. An estimate of the minimum amount of unsaturated
787 fatty acid required for growth of *Escherichia coli*. J Biol Chem. 1973;248(4):1188-95.
788 64. Feng Y, Cronan JE. Complex binding of the FabR repressor of bacterial
789 unsaturated fatty acid biosynthesis to its cognate promoters. Mol Microbiol.
790 2011;80(1):195-218.
791 65. Feng Y, Cronan JE. *Escherichia coli* unsaturated fatty acid synthesis: Complex
792 transcription of the *fabA* gene and *in vivo* identification of the essential reaction
793 catalyzed by FabB. Journal of Biological Chemistry. 2009;284(43):29526-35.
794 66. Henry MF, Cronan JE. *Escherichia coli* transcription factor that both activates
795 fatty acid synthesis and represses fatty acid degradation. Journal of Molecular Biology.
796 1991;222(4):843-9.
797 67. Henry MF, Cronan JE. A new mechanism of transcriptional regulation: Release of
798 an activator triggered by small molecule binding. Cell. 1992;70(4):671-9.
799 68. Rock CO, Jackowski S. Pathways for the incorporation of exogenous fatty acids
800 into phosphatidylethanolamine in *Escherichia coli*. J Biol Chem. 1985;260(23):12720-4.

801 69. Heath RJ, Rock CO. Roles of the FabA and FabZ β-hydroxyacyl-acyl carrier protein
802 dehydratases in *Escherichia coli* fatty acid biosynthesis. Journal of Biological Chemistry.
803 1996;271(44):27795-801.
804 70. Ostrander DB, Sparagna GC, Amoscato AA, McMillin JB, Dowhan W. Decreased
805 Cardiolipin Synthesis Corresponds with Cytochromec Release in Palmitate-induced
806 Cardiomyocyte Apoptosis. Journal of Biological Chemistry. 2001;276(41):38061-7.
807 71. Lewis RNAH, Zweytick D, Pabst G, Lohner K, McElhaney RN. Calorimetric, X-Ray
808 Diffraction, and Spectroscopic Studies of the Thermotropic Phase Behavior and
809 Organization of Tetramyristoyl Cardiolipin Membranes. Biophysical Journal.
810 2007;92(9):3166-77.
811 72. De Siervo AJ. Alterations in the phospholipid composition of *Escherichia coli* B
812 during growth at different temperatures. J Bacteriol. 1969;100(3):1342-9.
813 73. Bogdanov M, Sun J, Kaback HR, Dowhan W. A Phospholipid Acts as a Chaperone
814 in Assembly of a Membrane Transport Protein. Journal of Biological Chemistry.
815 1996;271(20):11615-8.
816 74. Mitchell AM, Silhavy TJ. Envelope stress responses: balancing damage repair and
817 toxicity. Nature Reviews Microbiology. 2019;17(7):417-28.
818 75. Luevano-Martinez LA, Kowaltowski AJ. Phosphatidylglycerol-derived
819 phospholipids have a universal, domain-crossing role in stress responses. Arch Biochem
820 Biophys. 2015;585:90-7.
821 76. Fernandez M, Paulucci NS, Peppino Margutti M, Biasutti AM, Racagni GE,
822 Villasuso AL, et al. Membrane Rigidity and Phosphatidic Acid (PtdOH) Signal: Two
823 Important Events in Acinetobacter guillouiae SFC 500-1A Exposed to Chromium(VI) and
824 Phenol. Lipids. 2019;54(9):557-70.
825 77. Shibata A, Ikawa K, Shimooka T, Terada H. Significant stabilization of the
826 phosphatidylcholine bilayer structure by incorporation of small amounts of cardiolipin.
827 Biochimica et Biophysica Acta (BBA) - Biomembranes. 1994;1192(1):71-8.
828 78. Boscia AL, Treece BW, Mohammadyani D, Klein-Seetharaman J, Braun AR,
829 Wassenaar TA, et al. X-ray structure, thermodynamics, elastic properties and MD
830 simulations of cardiolipin/dimyristoylphosphatidylcholine mixed membranes. Chemistry
831 and Physics of Lipids. 2014;178:1-10.
832 79. Pennington ER, Fix A, Sullivan EM, Brown DA, Kennedy A, Shaikh SR. Distinct
833 membrane properties are differentially influenced by cardiolipin content and acyl chain
834 composition in biomimetic membranes. Biochimica et Biophysica Acta (BBA) -
835 Biomembranes. 2017;1859(2):257-67.
836 80. Lopes SC, Ivanova G, de Castro B, Gameiro P. Revealing cardiolipins influence in
837 the construction of a significant mitochondrial membrane model. Biochimica et
838 Biophysica Acta (BBA) - Biomembranes. 2018;1860(11):2465-77.
839 81. Marr AG, Ingraham JL. Effect of temperature on the composition of fatty acids in
840 *Escherichia coli*. Journal of Bacteriology. 1962;84(6):1260-7.

841 82. Garwin JL, Klages AL, Cronan JE. Beta-ketoacyl-acyl carrier protein synthase II of
842 *Escherichia coli*. Evidence for function in the thermal regulation of fatty acid synthesis.
843 Journal of Biological Chemistry. 1980;255(8):3263-5.
844 83. de Mendoza D, Klages Ulrich A, Cronan JE. Thermal regulation of membrane
845 fluidity in *Escherichia coli*. Effects of overproduction of beta-ketoacyl-acyl carrier protein
846 synthase I. Journal of Biological Chemistry. 1983;258(4):2098-101.
847 84. Knapp BD, Huang KC. The effects of temperature on cellular physiology. Annual
848 Review of Biophysics. 2022;51(1):499-526.
849 85. Bogdanov M, Umeda M, Dowhan W. Phospholipid-assisted refolding of an
850 integral membrane protein: Minimum structural features for phosphatidylethanolamine
851 to act as a molecular chaperone. Journal of Biological Chemistry. 1999;274(18):12339-
852 45.
853 86. Raetz CR, Whitfield C. Lipopolysaccharide endotoxins. Annu Rev Biochem.
854 2002;71:635-700.
855 87. Conway T, Creecy JP, Maddox SM, Grissom JE, Conkle TL, Shadid TM, et al.
856 Unprecedented high-resolution view of bacterial operon architecture revealed by RNA
857 sequencing. mBio. 2014;5(4):e01442-14.
858 88. Thomason MK, Bischler T, Eisenbart SK, Förstner KU, Zhang A, Herbig A, et al.
859 Global transcriptional start site mapping using differential RNA sequencing reveals novel
860 antisense rnas in *Escherichia coli*. Journal of Bacteriology. 2015;197(1):18-28.
861 89. Adams PP, Baniulyte G, Esnault C, Chegireddy K, Singh N, Monge M, et al.
862 Regulatory roles of *Escherichia coli* 5' UTR and ORF-internal RNAs detected by 3' end
863 mapping. eLife. 2021;10:e62438.
864 90. Karp PD, Ong WK, Paley S, Billington R, Caspi R, Fulcher C, et al. The EcoCyc
865 database. EcoSal Plus. 2018;8(1):10.1128/ecosalplus.ESP-0006-2018.
866 91. Huerta AM, Collado-Vides J. Sigma70 promoters in *Escherichia coli*: specific
867 transcription in dense regions of overlapping promoter-like signals. Journal of Molecular
868 Biology. 2003;333(2):261-78.
869 92. Dowhan W, Bogdanov M. Lipid-dependent membrane protein topogenesis. Annu
870 Rev Biochem. 2009;78:515-40.
871 93. Bogdanov M, Xie J, Heacock P, Dowhan W. To flip or not to flip: lipid-protein
872 charge interactions are a determinant of final membrane protein topology. J Cell Biol.
873 2008;182(5):925-35.
874 94. Bogdanov M, Dowhan W. Lipid-dependent generation of dual topology for a
875 membrane protein. J Biol Chem. 2012;287(45):37939-48.
876 95. Bogdanov M, Dowhan W, Vitrac H. Lipids and topological rules governing
877 membrane protein assembly. Biochim Biophys Acta. 2014;1843(8):1475-88.
878 96. Ramezanifard R, Golubeva YA, Palmer AD, Slauch JM. TamAB is regulated by
879 PhoPQ and functions in outer membrane homeostasis during *Salmonella* pathogenesis. J
880 Bacteriol. 2023;205(10):e0018323.
881 97. Szklarczyk D, Gable AL, Nastou KC, Lyon D, Kirsch R, Pyysalo S, et al. The STRING
882 database in 2021: customizable protein-protein networks, and functional

883 characterization of user-uploaded gene/measurement sets. Nucleic Acids Res.
884 2021;49(D1):D605-d12.
885 98. Grasekamp KP, Beaud B, Taib N, Audrain B, Bardiaux B, Rossez Y, et al. Bridges
886 instead of boats? The Mla system of diderm Firmicute *Veillonella parvula* reveals an
887 ancestral transenvelope core of phospholipid trafficking. bioRxiv.
888 2023:2023.06.30.547184.
889 99. Baba T, Ara T, Hasegawa M, Takai Y, Okumura Y, Baba M, et al. Construction of
890 *Escherichia coli* K-12 in-frame, single-gene knockout mutants: the Keio collection. Mol
891 Syst Biol. 2006;2:2006.0008-2006.0008.
892 100. Silhavy TJ, Berman ML, Enquist LW. Experiments with gene fusions: Cold Spring
893 Harbor Laboratory; 1984.
894 101. Datsenko KA, Wanner BL. One-step inactivation of chromosomal genes in
895 *Escherichia coli* K-12 using PCR products. Proceedings of the National Academy of
896 Sciences. 2000;97(12):6640-5.
897 102. MacRitchie DM, Ward JD, Nevesinjac AZ, Raivio TL. Activation of the Cpx
898 envelope stress response down-regulates expression of several locus of enterocyte
899 effacement-encoded genes in enteropathogenic *Escherichia coli*. Infect Immun.
900 2008;76(4):1465-75.
901 103. Wong JL, Vogt SL, Raivio TL. Using reporter genes and the *Escherichia coli* ASKA
902 overexpression library in screens for regulators of the Gram negative envelope stress
903 response. Methods Mol Biol. 2013;966:337-57.
904 104. Deatherage DE, Barrick JE. Identification of mutations in laboratory-evolved
905 microbes from next-generation sequencing data using breseq. Methods Mol Biol.
906 2014;1151:165-88.
907 105. Bailey TL, Elkan C. Fitting a mixture model by expectation maximization to
908 discover motifs in biopolymers. Proc Int Conf Intell Syst Mol Biol. 1994;2:28-36.
909 106. Bailey TL, Johnson J, Grant CE, Noble WS. The MEME Suite. Nucleic Acids Res.
910 2015;43(W1):W39-49.
911 107. Singer M, Baker TA, Schnitzler G, Deischel SM, Goel M, Dove W, et al. A
912 collection of strains containing genetically linked alternating antibiotic resistance
913 elements for genetic mapping of Escherichia coli. Microbiol Rev. 1989;53(1):1-24.
914 108. Rai AK, Carr JF, Bautista DE, Wang W, Mitchell AM. ElyC and cyclic
915 enterobacterial common antigen regulate synthesis of phosphoglyceride-linked
916 enterobacterial common antigen. mBio. 2021;12(6):e02846-21.
917 109. Kim D, Paggi JM, Park C, Bennett C, Salzberg SL. Graph-based genome alignment
918 and genotyping with HISAT2 and HISAT-genotype. Nature Biotechnology.
919 2019;37(8):907-15.
920 110. Liao Y, Smyth GK, Shi W. featureCounts: an efficient general purpose program for
921 assigning sequence reads to genomic features. Bioinformatics. 2013;30(7):923-30.
922 111. Robinson MD, McCarthy DJ, Smyth GK. edgeR: a Bioconductor package for
923 differential expression analysis of digital gene expression data. Bioinformatics.
924 2009;26(1):139-40.

925 112. Ritchie ME, Phipson B, Wu D, Hu Y, Law CW, Shi W, Smyth GK. limma powers
926 differential expression analyses for RNA-sequencing and microarray studies. Nucleic
927 Acids Research. 2015;43(7):e47-e.
928 113. Sparagna GC, Johnson CA, McCune SA, Moore RL, Murphy RC. Quantitation of
929 cardiolipin molecular species in spontaneously hypertensive heart failure rats using
930 electrospray ionization mass spectrometry. J Lipid Res. 2005;46(6):1196-204.
931 114. Hryc CF, Mallampalli VKPS, Bovshik EI, Azinas S, Fan G, Serysheva II, et al.
932 Structural insights into cardiolipin replacement by phosphatidylglycerol in a cardiolipin-
933 lacking yeast respiratory supercomplex. Nature Communications. 2023;14(1):2783.

934
935

936 **Figures and Tables**

937

938

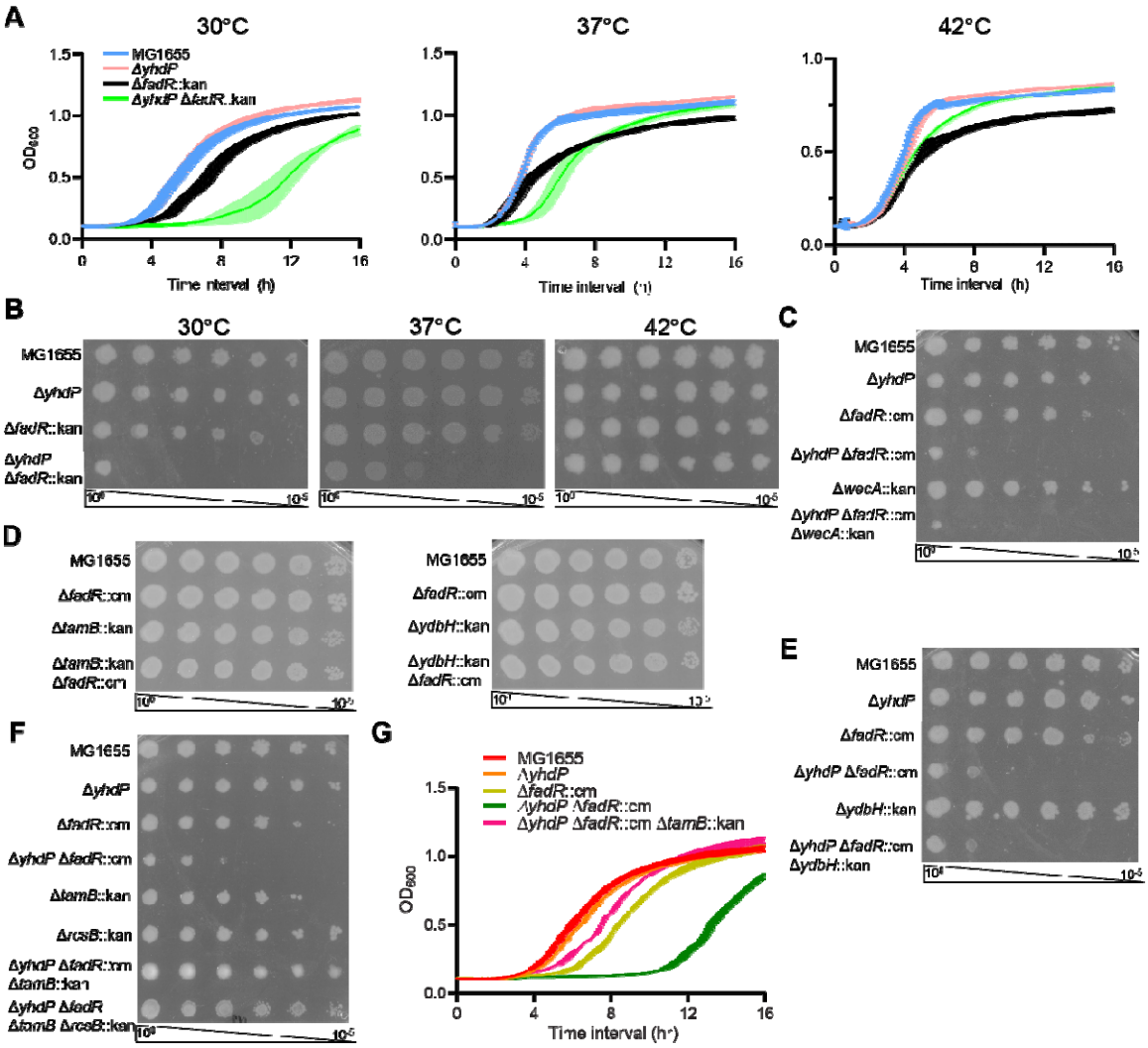

939

940 **Figure 1. Deletion of *yhdP* and *fadR* causes synthetic cold sensitivity for which TamB is**
941 **necessary. (A)** The Δ*yhdP* Δ*fadR* strain had impaired growth at lower temperatures. **(B)**
942 EOPs were performed to confirm the growth defect of the Δ*yhdP* Δ*fadR* strain. **(C-F)**
943 EOPs were performed at 30 °C to assess cold sensitivity. **(C)** The growth of the Δ*yhdP*
944 Δ*fadR* strain was not affected by the loss of ECA (Δ*wecA*). **(D)** Neither a Δ*tamB* Δ*fadR*
945 strain nor a Δ*ydbH* Δ*fadR* strain exhibited cold sensitivity. **(E)** Deletion of *ydbH* did not
946 suppress cold sensitivity in the Δ*yhdP* Δ*fadR* strain. **(F)** Deletion of *tamB* completely
947 suppressed cold sensitivity in the Δ*yhdP* Δ*fadR* strain and the Rcs stress response was
948 not necessary for this suppression. **(G)** Growth curves were performed at 30 °C . The
949 Δ*yhdP* Δ*fadR* Δ*tamB* strain grew well, indicating suppression was unlikely to result from
950 slow growth. Quantitative data are shown as the mean of three biological replicates ±
951 the SEM. Images are representative of three independent experiments.

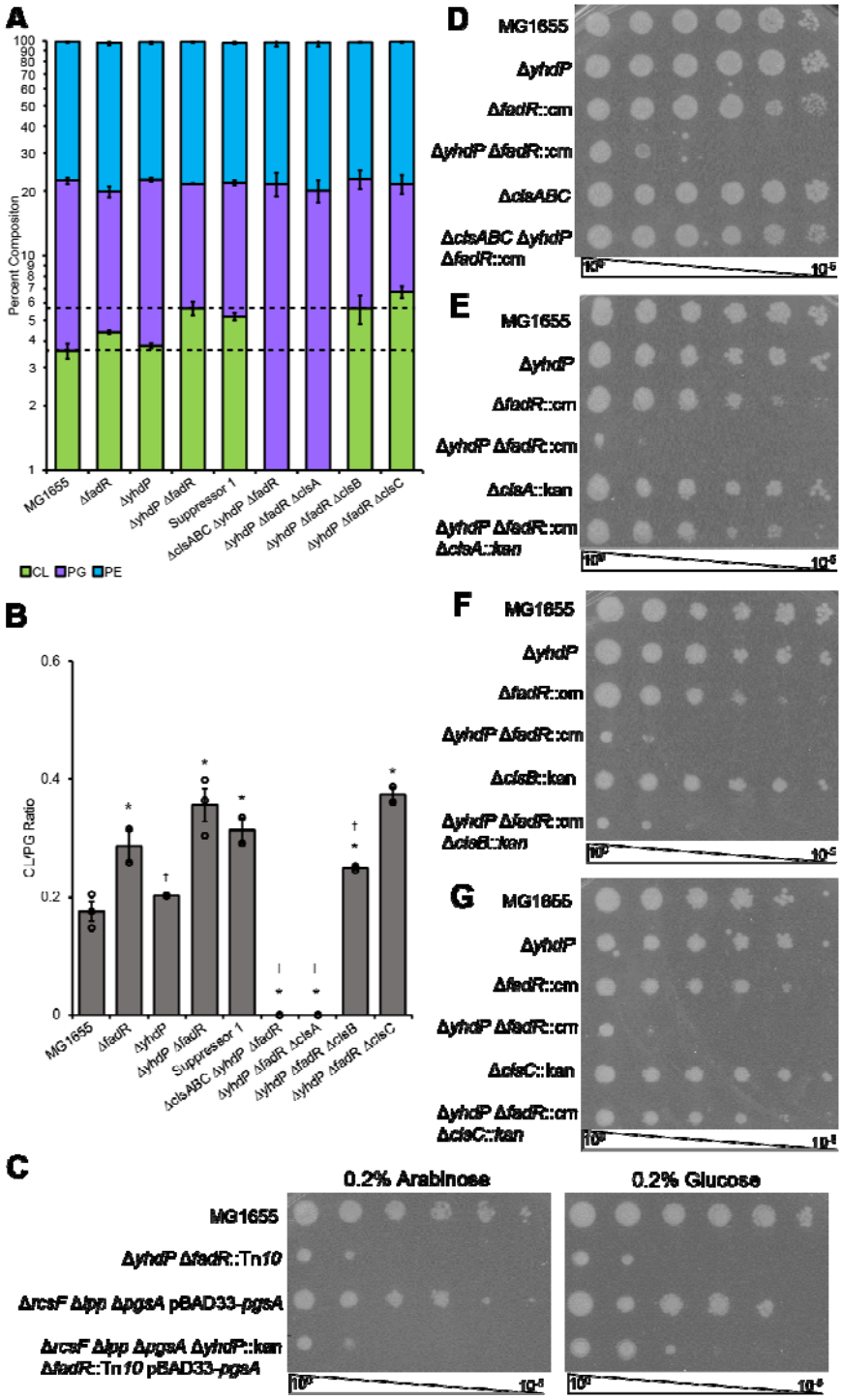

Figure 2. Lowering cardiolipin levels can suppress cold sensitivity of the Δ*yhdP* Δ*fadR* strain. (A-B) Thin layer chromatography (TLC) of lipid extracts was performed for the indicated cultures grown to log phase at 42 °C then transferred to 30 °C for 2 hours before analysis. **(A)** Relative phospholipid levels were calculated. The Δ*yhdP* Δ*fadR* strain

959 shows increased levels of CL and a concomitant decrease in PG levels, increasing the
960 ratio of CL to PG (B). Data are averages of two to three biological replicates ± the SEM.
961 For ratios individual data points are indicated with open circles. * $p<0.05$ vs. MG1655 by
962 Student's T-test; ‡ $p<0.05$ vs. the Δ*yhdP* Δ*fadR* strain by Student's T-test. **(C-G)** Growth
963 effects of altered phospholipid levels were investigated by EOP. Images are
964 representative of three independent experiments. **(C)** PgsA depletion strains in a
965 background where *pgsA* is non-essential were used to assay the effect of lowering PG
966 and CL levels on cold sensitivity. Arabinose induces expression of *pgsA* while glucose
967 represses. Cultures were induced or repressed for 4-5 generations before as well as
968 during the EOP. Lowering PG and CL levels partially suppressed cold sensitivity. **(D)**
969 Deletion of the three CL synthases, *clsA*, *clsB*, and *clsC*, suppressed cold sensitivity of the
970 Δ*yhdP* Δ*fadR* strain. **(E)** Deletion of *clsA* also suppressed cold sensitivity. **(F)** Deletion of
971 *clsB* does not suppress cold sensitivity, while deletion of *clsC* (F) does.
972
973

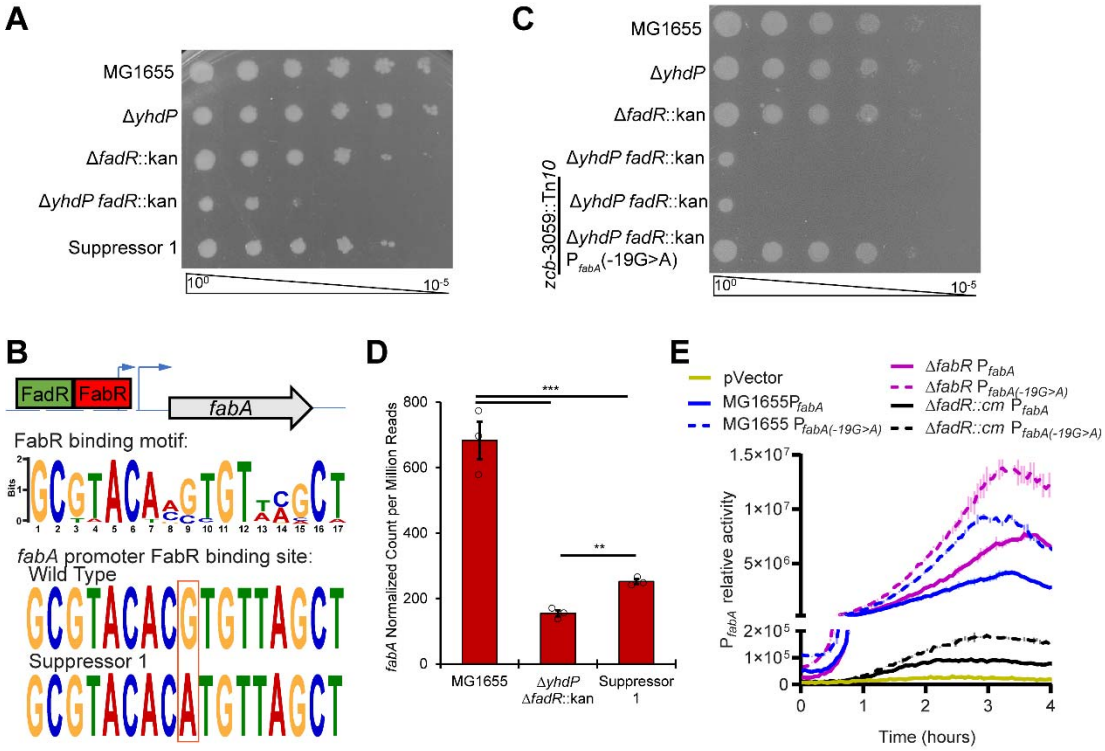

Figure 3. Cold sensitivity can be suppressed by increasing *fabA* expression. (A) The cold sensitivity of a spontaneous suppressor of Δ*yhdP* Δ*fadR* cold sensitivity was tested by EOP. The suppressor returned growth to the level of the Δ*fadR* mutant. **(B)** A diagram of the promoter region of *fabA* is shown with its transcriptional start sites (blue arrows) and regulator binding sites (boxes). FadR acts as an activator while FabR acts as a repressor. The motif of the FabR binding site, generated using MEME, is shown with the sequences of the parent strain and of Suppressor 1. **(C)** The P_{fabA}(-19G>A) mutation was linked to a Tn*10* and transferred to the Δ*yhdP* Δ*fadR* strain by transduction. The Δ*yhdP* Δ*fadR* strain with P_{fabA}(-19G>A) was not cold sensitivity, confirming suppression. **(D)** *fabA* RNA levels are shown. Bars are the mean of three biological replicates ± the SEM. Individual data points are shown as open circles. ** $p<0.005$, *** $p<0.0005$ by quasi-linear F-test. Data are from the RNA-seq experiment in Figure 5 and *fabA* data are also shown in Figure 5F. **(E)** Luciferase reporters of wild-type and mutant *fabA* promoter activity were constructed. The mutation caused similar fold increases in P_{fabA} activity in all strain backgrounds, indicating the activity of the second *fabA* promoter and not FabR binding were likely affected by the suppressor mutation. Data are luminescence relative to OD_{600} and are shown as the average of two biological replicates ± the SEM.

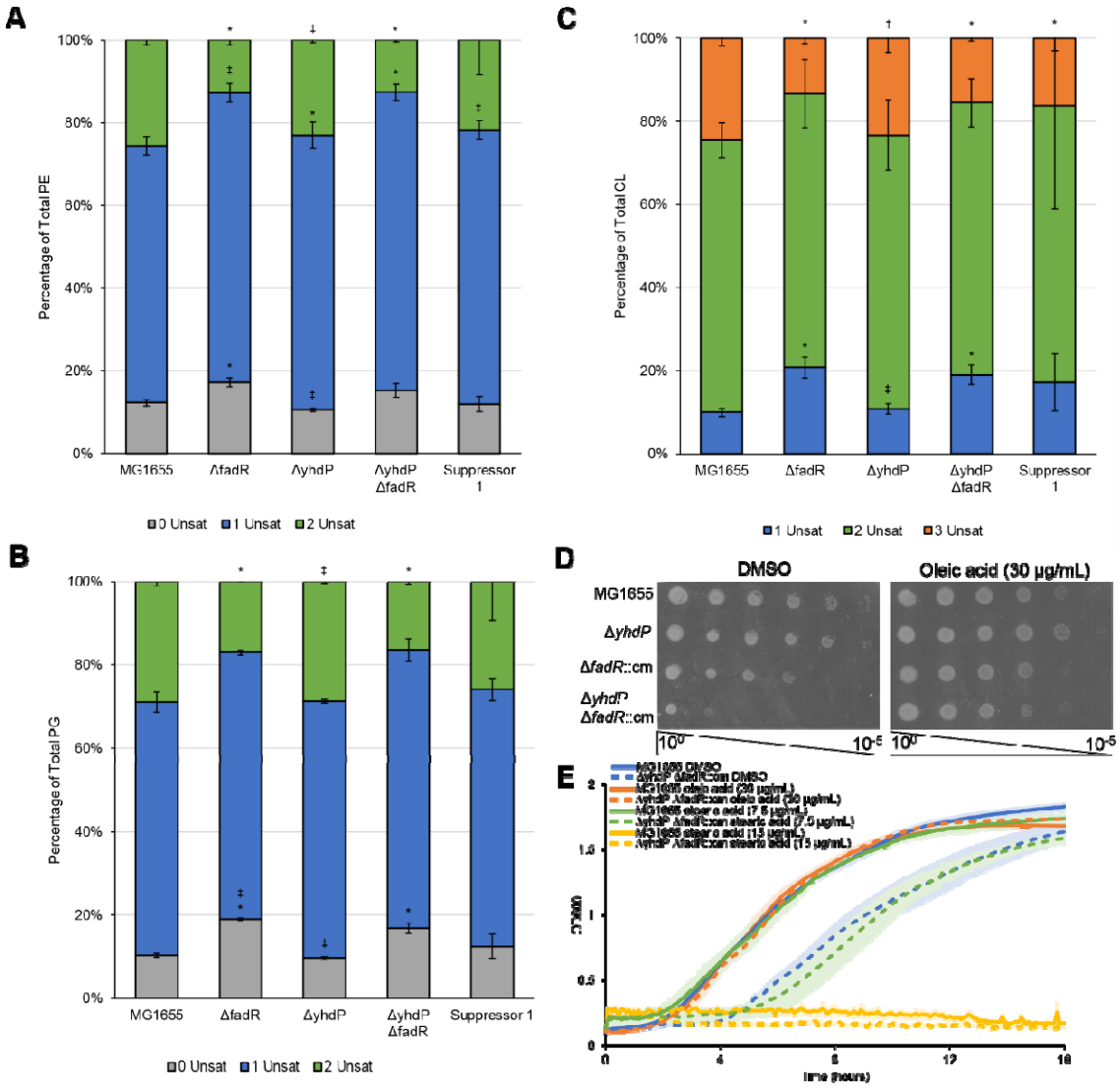

Figure 4. Decreasing fatty acid saturation suppresses Δ*yhdP* Δ*fadR* cold sensitivity. (A-C) Lipid were extracted from cells grown to OD_{600} 0.2 at 42 °C then shifted to 30 °C for 2 hours before harvest. LC/MS was performed on lipid extracts using absolute quantification and the percentage of each specific species of PE (A), PG (B), and CL (C) was calculated using the sum of all molecular species detected. Suppressor 1 trends towards decreased saturation compared to its parent strain (Δ*yhdP* Δ*fadR*). Data for phospholipids without unsaturations are shown in grey, with one unsaturation in blue, with two unsaturations in green, with three unsaturations in orange. Data are the average of three biological replicates ± the SEM. * $p<0.05$ vs. MG1655 by the Mann-Whitney test; ‡ $p<0.05$ vs. the Δ*yhdP* Δ*fadR* strain by the Mann-Whitney test. All molecular species are shown in Fig. S6. **(D)** EOPS were performed on media supplemented with oleic acid or a vehicle control. Oleic acid suppresses the cold sensitivity of the Δ*yhdP* Δ*fadR* strain. **(E)** Growth curves of the indicated strains were

1008 performed in the presence of oleic acid, stearic acid, or a vehicle control. Oleic acid
1009 suppressed the cold sensitivity of the Δ*yhdP* Δ*fadR* strain while stearic acid did not. Data
1010 are the average of three biological replicates ± the SEM.
1011

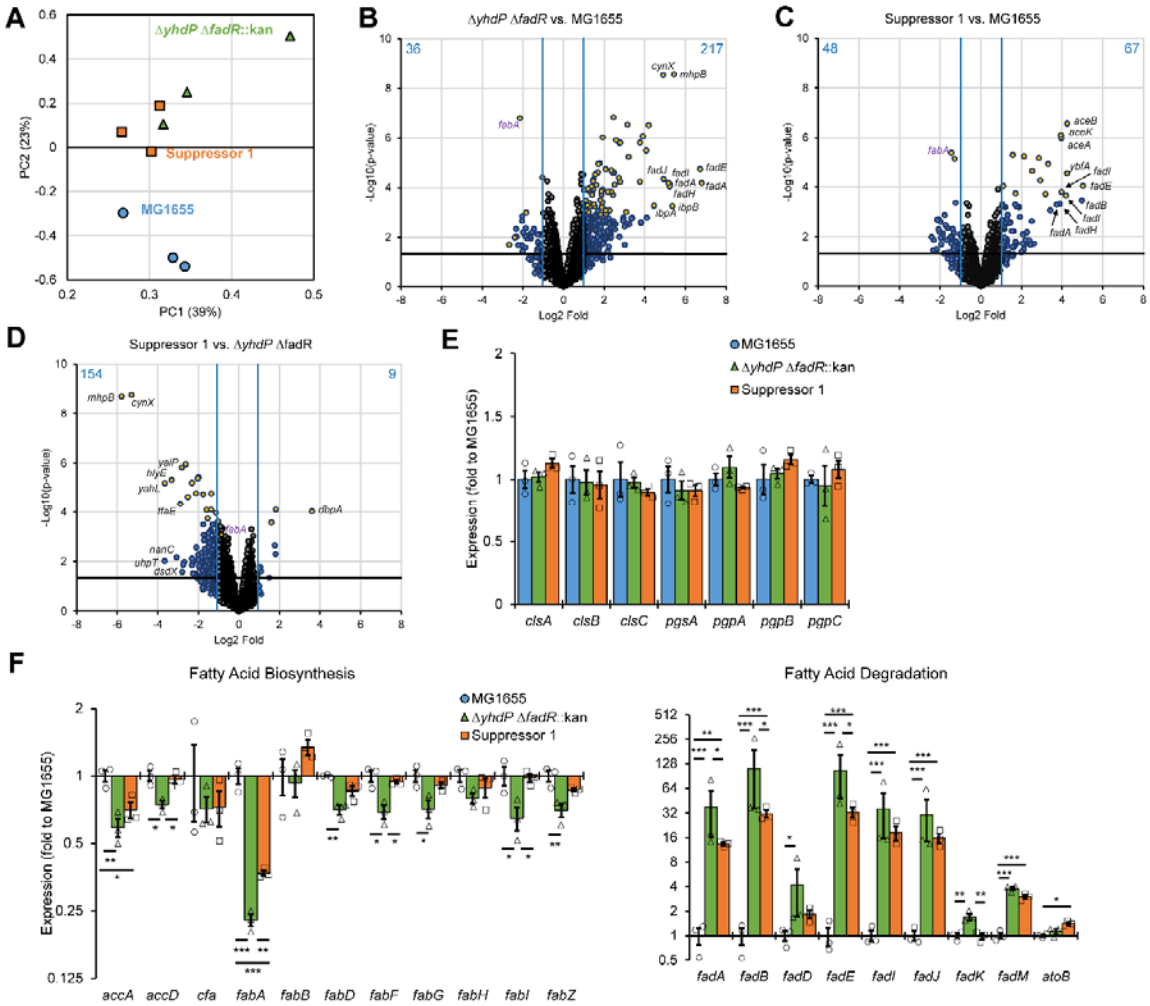

Figure 5. Transcriptional landscape of the Δ*yhdP* Δ*fadR* and suppressed strain. Three biological replicates of the indicated strains were grown at 42 °C to mid-log then transferred to 30 °C for 30 minutes before harvesting RNA and performing RNA-seq. Differential expression was calculated based on a greater than 2-fold change in expression and a p value of less than 0.05 by quasi-linear F-test. **(A)** PCA was performed on the expression of all genes differentially expressed between any groups of samples. Suppressor 1 and the Δ*yhdP* Δ*fadR* strain grouped closer together than to the wild-type strain, although Suppressor 1 was closer to wild type than the Δ*yhdP* Δ*fadR* strain. **(B-D)** Volcano plots show the average fold change and significance of expression changes between the Δ*yhdP* Δ*fadR* strain and wild-type MG1655 (B), Suppressor 1 and wild-type MG1655 (C), and Suppressor 1 and the Δ*yhdP* Δ*fadR* strain (D). Genes with changes greater than 2-fold are shown in blue, while genes with changes less than 2-fold are shown in grey. Genes with a q-value (false discovery rate) of less than 0.05 are shown in yellow. Blue lines indicate a 2-fold change and dotted line indicates p>0.05. The number of up or down regulated genes is indicated in blue. The names of the 10 genes with the largest changes are called out. More genes were up-regulated then down regulated in the Δ*yhdP* Δ*fadR* strain and Suppressor 1 vs. wild type. More genes were down

1030 regulated in Suppressor 1 compared to the Δ*yhdP* Δ*fadR* strain. **(E)** Relative expression
1031 of genes in the CL synthesis pathway is shown as averages ± the SEM and individual data
1032 points. No significant changes were evident. **(F)** Relative expression of genes in the fatty
1033 acid synthesis and degradation pathways is shown as averages ± the SEM and individual
1034 data points. A general normalizing of these pathways occurred in Suppressor 1
1035 compared to the Δ*yhdP* Δ*fadR* strain; however, the most significant change was in the
1036 expression of *fabA*. * $p<0.05$, ** $p<0.005$, *** $p<0.0005$ by quasi-linear F-test.
1037

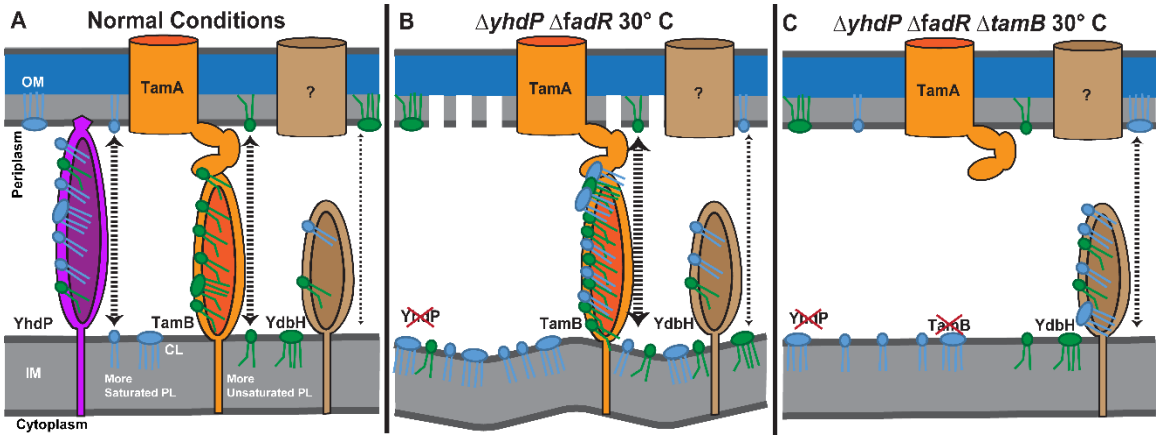

Figure 6. Hypothesized model for the role of YhdP and TamB in phospholipid transport. Our data can be explained by the following model of phospholipid transport. **(A)** In normal conditions, YhdP is mainly responsible for the transport of phospholipids with more saturated fatty acid chains between the IM and OM. TamB shows a strong preference for transporting phospholipids with more unsaturated fatty acids, with YdbH playing a minor role in phospholipid transport. **(B)** In the Δ*yhdP* Δ*fadR* strain, YhdP is not available to transport more saturated phospholipids and the proportion of both saturated fatty acids and cardiolipin is increased, especially at low temperature. The fluidity of the membrane is also lessened by the low temperature. In these conditions, transport of phospholipids between the membranes is impeded, due to clogging of TamB by a combination of less saturated phospholipids and/or bulky and highly disordered CL. This leads to a lethal lack of phospholipids in the OM and overabundance of phospholipids in the IM. **(C)** When *tamB* is deleted in the Δ*yhdP* Δ*fadR* strain, the clogging of TamB is relieved, and the cell relies on YdbH for phospholipid transport overcoming the cold sensitivity. PL: phospholipid